THE EFFECT OF ELECTROSTATIC FIELDS ON THE ORIENTATION OF COLLOIDAL PARTICLES IMMERSED IN SHEAR FLOW

Thesis by

Sterge T. Demetriades, A.B., M.S.

In Partial Fulfillment of the Requirements

For the Degree of

Mechanical Engineer

California Institute of Technology

Pasadena, California

1958

ACKNOWLEDGMENT

The author is indebted to Professor J. H. Wayland for his support during the course of this investigation.

ABSTRACT

The orientation distribution function for colloidal particles immersed in Couette flow with an electric field parallel to the velocity gradient is derived in this study. A description of a modified and improved version of streaming birefringence apparatus built to test this theory and to conduct other studies in streaming birefringence is also included.

TABLE OF CONTENTS

CHAPTER	PAGE

LIST OF FIGURES

LIST OF SYMBOLS

A = $\frac{M}{\sin 2\lambda} = \frac{2K}{\cos 2\lambda}$, defined in figure 5 and equation 36.

A_x, A_y, A_z = symbols defined in Appendix D.

a,b,c = dimensions of the semiaxes of the ellipsoidal particle.

a_1, b_1, c_1 = components of distortion of fluid defined by equation 8.

$a_{nm,j}$;$b_{nm,j}$ = general coefficients of F_j series, see equation 40.

B = a constant defined in Appendix C.

D = orientational diffusion coefficient (rotary diffusion coefficient according to some authors), $\sec^{-1}$.

E = electric field strength, volt/cm.

E_1, E_2 = resultant fields inside particle when its major axis is normal and parallel to field, Appendix C.

$\vec{E}$ = electric field vector.

f_1,g_1,h_1,f_2,g_2,h_2 = components of distortion and rotation defined by equation 8 and Appendix D.

F = orientational distribution function, i.e. a function giving the distribution of orientations of the major axis of the colloidal particles.

F_j = j^{th} term of series expansion of F, defined by equations 38 and 40.

G = velocity gradient, $\sec^{-1}$.

K = $\frac{1}{4} G^2 \left(\frac{a^2 - b^2}{a^2 + b^2}\right) = \frac{1}{4}$ GR, defined in figure 5.

K = $\varepsilon/\varepsilon_w$, defined in Appendix C.

L_E = resultant electrostatic torque defined in Appendix C.

L_{Ex},L_{Ey},L_{Ez} = components of electrostatic torque along x,y,z respectively.

L_H = resultant hydrodynamic torque.

L_{Hx},L_{Hy},L_{Hz} = components of hydrodynamic torque along x,y,z respectively.

L_x = $L_{Hx} + L_{Ex}$, resultant couple along x-axis.

L_y = $L_{Hy} + L_{Ey}$, resultant couple along y-axis.

L_z = $L_{Hz} + L_{Ez}$, resultant couple along z-axis.

M = $A_y\left(\frac{BE^2}{a^2+b^2}\right)$, defined in figure 5.

p = pressure in appropriate units.

P_{2n} = Legendre polynomials, $P_0(x) = P_0(\cos\theta) = 1$, etc.

P_{2n}^{2m} = Legendre functions, $P_2^2(x) = P_2^2(\cos\theta) = \frac{3}{2}(1 - \cos\theta) = 3(1 - x^2)$, etc.

R = $\frac{a^2 - b^2}{a^2 + b^2}$; a is the semimajor axis.

s = $a(a^2 - b^2)^{-1/2}$, defined in Appendix C.

S_0 = $(K - 1)s[(1 - s^2)\coth^{-1}s + s]$, defined in Appendix C.

u, v, w = velocity components of the fluid at any point.

u_0, v_0, w_0 = the three components of the undisturbed motion of the fluid in the neighborhood of the particle.

u_0',v_0',w_0' = the three components of the undisturbed motion of the fluid far from the particle along x',y' and z' axes respectively.

x, y, z = system of axes fixed in the particle and rotating with it.

x', y', z' = system of axes fixed in direction in the cylinder system with x' parallel to the axes of the cylinders.

x'',y'',z'';x''',y''',z''' = intermediate transformation axes shown in figures 1A to 3A (Appendix A).

α = ratio of velocity gradient to rotary diffusion coefficient, $\alpha = \frac{G}{D}$, dimensionless.

α = angle between the principal axis, x, of particle and the electrostatic field $\vec{E}$.

β = $\frac{A}{D} = \frac{\sqrt{4K^2 + M^2}}{D} = \frac{R}{D}\sqrt{\frac{1}{4} G^2 + \frac{B^2E^4}{A_y^{\,2}(a^2 - b^2)^2}}$, expansion parameter, dimensionless.

γ = $\varphi - \lambda$.

δ = δ'.

δ' = the smallest angle between the torque L_E and the x' axis on $x'z'$ plane.

δ'' = angle between the resultant electric torque L_E and the $+ x'$ axis, measured counterclockwise from $+ x'$ axis.

Δn = magnitude of birefringence, i.e. phase difference of the elliptically polarized light emerging from the cylinder system or $\Delta n = n_z - n_x$ where n_z, n_x are the principal indices of refraction of the flowing solution.

ε, ε_w = capacitivity of vacuum and water respectively.

θ, φ, ψ = Euler angles produced by transformations of Appendix A.

$\dot{\theta}$, $\dot{\varphi}$, $\dot{\psi}$ = time derivatives of Euler angles.

$\vec{\theta}_1$, $\vec{\varphi}_1$ = unit vectors along θ and φ coordinates.

λ = angle defined in figure 5, $\sin 2\lambda = \frac{M}{A}$, $\cos 2\lambda = \frac{2K}{A}$.

φ' = angle by which the extinction angle deviates from 45°, i.e. $x = 45^\circ - \varphi'$, where χ is the angle of extinction.

μ = viscosity of fluid in appropriate units.

ρ = density of fluid, gm/cm^3.

ω_1, ω_2, ω_3 = spins of the ellipsoid about its axis.

$\vec{\omega}$ = angular flux, sec^{-1}, defined by equation 28.

Ω = solid angle.

I. INTRODUCTION

An attempt is made in this study to determine theoretically the effect of electric fields on the orientation of colloidal particles in shear flow. The experimental verification of the theoretical results has not been completed because the alloted time was all spent on the design, construction and assembly of the complex equipment required for the experiment. Double refraction (birefringence) was considered and chosen as the most appropriate method for the experimental study of this effect. Therefore the problem investigated in detail is one which is relatively easy to study in concentric-cylinder streaming-birefringence apparatus, namely the case when the electric field is parallel to the velocity gradient. Thus it would seem more appropriate to qualify the title further to read "The Effect of an Electric Field Normal to the Velocity on the Orientation of Colloidal Particles in Couette Flow".

Streaming birefringence (SBR)* has already become an important biochemical and hydrodynamic research tool. Its biochemical uses are outlined in the excellent general review by Cerf and Scheraga (1). Although Humphry (2) was first to suggest the use of SBR as a hydrodynamic research tool, Wayland (3) was first to carry out the quantitative determination of a complex flow field by means of SBR measurements.

---

*SBR = streaming birefringence = double refraction associated with shear flow = flow birefringence. If an external field is applied to a normally isotropic pure liquid, solution or suspension, the system in most cases becomes birefringent. The production of double refraction in this manner is referred to as the Kerr effect, the Cotton-Mouton effect, or the Maxwell effect, depending upon whether the applied field is electric, magnetic or hydrodynamic, respectively.

He found that quantitative measurements were possible as close as 0.1 mm from a wall. In addition, Wayland (3) presents an excellent review of the hydrodynamic uses of SBR. More recently Prados and Peebles (4) attempted an analysis of two-dimensional laminar flow utilizing a doubly refracting liquid. A comprehensive literature survey of SBR was presented by Peebles, Prados and Honeycutt (5). It appears therefore that the effect of shear fields on the orientation of colloidal particles has been the subject of numerous and extensive investigations.

Electric birefringence has been applied with success to the study of static suspensions of colloidal particles by many (e.g. Benoit (6,7), O'Konski and Zimm (8), O'Konski and Haltner (9)) and the effect of electric fields on the orientation and relaxation effects of colloidal particles in suspensions is well-known.

By contrast, the effect of a simultaneous application of electric and shear fields on the orientation of colloidal particles, isotropic pure liquids or solutions has received scant attention. At this date Tolstoi (10) appears to be the only investigator to have studied the combined Kerr and Maxwell effects. He considered the effect of a simultaneous application of electric and hydrodynamic fields on a particle having an anisotropic polarizability but no permanent dipole moment. He investigated the case when the electric field, $\vec{E}$, is applied in the direction of the velocity gradient (i.e. normal to the flow velocity) and he claims that by generalizing the results of Peterlin and Stuart (11, 12) for small α (α = ratio of the velocity gradient to the rotary diffusion constant), he found that the extinction angle is not 45° as α approaches zero but deviates from 45° by an amount φ' where

$$\tan 2\varphi' = \frac{2 \tan \varphi'}{1 - \tan^2 \varphi'} \sim \frac{E^2}{G} . \qquad (1)$$

The quantity G in equation 1 is the velocity gradient. In addition he gave an expression for the dependence of the birefringence on E and G, which may be written in the form:

$$\left.\frac{\partial(\Delta n)}{\partial(E^2)}\right|_{\substack{E=0\\G=\text{constant}}} = 0. \qquad (2)$$

Tolstoi (10) applied these results for colloidal suspensions to the limiting case of pure liquids. Without elaborating on his method and results he states that equations 1 and 2 were found to hold for a sample of purified transformer oil. By introducing the effect of the electric field into the Raman and Krishnan (13) theory for pure liquids, he obtained the following equations:

$$\frac{2 \tan \varphi'}{1 - \tan \varphi'} \sim \frac{E^2}{G} \qquad (3)$$

and

$$\left.\frac{\partial(\Delta n)}{\partial(E^2)}\right|_{\substack{E=0\\G=\text{constant}}} \neq 0. \qquad (4)$$

Equations 3 and 4 are in disagreement with the experiments just mentioned. Therefore, Tolstoi concluded that the experiments were in agreement with an orientation-type theory (Peterlin and Stuart, (11,12)) and in disagreement with the Raman and Krishnan theory. The disagreement of the latter theory with experiments on pure liquids had also been indicated earlier by Sadron (14, 15). A summary of Tolstoi's study appears in English in the comprehensive review paper of Cerf and Sheraga (1).

Since Tolstoi does not derive an expression for the orientation-distribution function in terms of the angles θ and φ and does not provide an exact expression for the angle of extinction or the amount of birefringence as a function of the field strengths and particle properties, it is impossible to evaluate the merits of the combined Kerr and Maxwell effects as a hydrodynamic or biochemical research tool on the basis of his work alone. In fact it appears that Tolstoi considered only the two-dimensional problem, i.e. when $\theta = 90^\circ$ = constant, so that the major axis of all his particles lies completely on the plane which contains the flow velocity vector and the electric field vector. Therefore, in order to determine the usefulness of this combined-field method it is necessary to develop the theory of the orientation of colloidal particles in Couette flow with an electric field normal to the velocity vector. The theoretical results of this investigation appear below.

A description of the experimental apparatus and procedures is given in Appendix F.

II. EFFECT OF AN ELECTRIC FIELD NORMAL TO THE FLOW VELOCITY ON ORIENTATION OF COLLOIDAL PARTICLES IN COUETTE FLOW

The success of a theory to account for or predict experimental observations depends ultimately on the model proposed for the solute particles and the simplifying assumptions made in order to treat rigorously their interaction with the hydrodynamic and electric fields. It is appropriate therefore at this point to outline the problem with special emphasis on the assumptions that will have to be made for its solution.

Perrin (16) has developed the theory of diffusion of orientation due to Brownian movement in the presence of an external orienting field. Now if the colloidal particles in question obey the general laws of Brownian movement, the orientation distribution function F obeys the general equation

$$D\nabla^2 F - \text{div}\ (F\vec{\omega}) = \frac{\partial F}{\partial t} \tag{5}$$

where D is the orientational diffusion coefficient (rotary diffusion coefficient according to most authors) and $\vec{\omega}$ is the angular flux of the particles in the absence of Brownian movement due to external orienting fields. Equation 5 is no more than a statement of the fact that the number of particles which attain a certain orientation due to Brownian movement per unit time minus the number of particles which lose that orientation due to the effect of the fields which generate $\vec{\omega}$, is the number of particles which accumulate in that orientation per unit time. When steady-state is attained in the absence of orienting fields all orientations are equally likely and normalization yields $F = \frac{1}{4\pi}$. The suspension then is isotropic. As soon as an external orienting field is applied, this equilibrium value of F is destroyed. The particles lose the uniform orientation imposed by Brownian movement. Subsequently, if the external fields reach a steady state then F reaches a new equilibrium and this new F with steady-state external fields is given (after the characteristics of the suspension have settled to a steady state) by

$$D\nabla^2 F - \operatorname{div}\,(F\vec{\omega}) = 0. \qquad (6)$$

The work of Sadron (15), Peterlin (17) and Peterlin and Stuart (11) proved that equation 6 holds for particles which are rigid ellipsoids of revolution in an orienting field of shear. The results of Peterlin and Stuart have been extended by Scheraga, Edsall and Gadd (18) to the region of high velocity gradient by means of a high-speed computer. Snellman and Björnstall (19) have also considered the effect of absorption on the observed phenomenon. For many of the synthetic polymers, however, the rigid model appears to be untenable. The work of Benoit (6), O'Konski and Zimm (8) and O'Konski and Haltner (9) established that equation 6 holds for particles which are rigid ellipsoids of revolution in an orienting electrostatic field.

It appears therefore that in cases where the particle is rigid, flow or electric birefringence gives information about its size and shape. In cases where it is not rigid these techniques can furnish information about the internal motion of the molecule (for further details on non-rigid particles see the excellent review article of Cerf and Scheraga (1)).

The angular flux $\vec{\omega}$ of the particles in the absence of Brownian movement is the parameter which feels the influence of the external orienting fields. Therefore the dynamic problem of the motion of these particles under the influence of these fields needs to be considered in detail.

In general we can decompose the system of forces acting on the particle into purely hydrodynamic and purely electric components the sum of which is equal to and opposes the forces acting on the fluid next to the particle.

Jeffery (20), treated the problem of rigid ellipsoids of revolution in a viscous fluid whose motion is laminar. He considered a system of axes x,y,z fixed in the particle and moving with it with center at the origin of the particle whose surface then is described by

$$\frac{x^2}{a^2} + \frac{y^2}{b^2} + \frac{z^2}{c^2} = 1. \tag{7}$$

The undisturbed motion of the fluid in the neighborhood of the particle is then given by

$$\left.\begin{aligned} u_0 &= a_1x + h_1y + g_1z + g_2z - h_2y \\ v_0 &= h_1x + b_1y + f_1z + h_2x - f_2y \\ w_0 &= g_1x + f_1y + c_1z + f_2y - g_2z \end{aligned}\right\} \tag{8}$$

where a_1, b_1, c_1, f_1, g_1, h_1, f_2, g_2, h_2 are the components of distortion and rotation of the fluid. These are assumed to be constant in space through a volume which is large compared with the dimensions of the particle. They will, however, vary with time, since the particle will rotate under the influence of the fluid and the axes x,y,z will be rotating axes.

Neglecting squares and products of the velocities, the equations of motion of an incompressible viscous fluid referred to moving axes are of the type

$$\mu\nabla^2 u - \frac{\partial p}{\partial x} = \rho\left\{ \frac{\partial u}{\partial t} - \omega_3 v + \omega_2 w\right\} \tag{9}$$

where ρ, μ, p are respectively the density, coefficient of viscosity and mean pressure of the fluid while ω_1, ω_2, ω_3, the spins of the ellipsoid about its axes, are produced by the motion of the fluid and, as Jeffery proves, are of the same order as the velocities u, v and w. Therefore for small u, v and w all products like $\omega_3 v$ may be neglected. Jeffery also proves that the remaining terms on the right-hand side of equation 9 are of the second order of small quantities (i.e. products of the type $\omega_1 \varepsilon_1$ where ε_1 and ω_1 are both small) and are therefore negligible. The equations of motion then reduce to

$$\mu\nabla^2 u = \frac{\partial p}{\partial x}, \quad \mu\nabla^2 v = \frac{\partial p}{\partial y} \quad \text{and} \quad \mu\nabla^2 w = \frac{\partial p}{\partial z}, \tag{10}$$

with the equation of continuity,

$$\frac{\partial u}{\partial x} + \frac{\partial v}{\partial y} + \frac{\partial w}{\partial z} = 0. \tag{11}$$

Jeffery then finds a solution of equations 10 and 11 which agree with equation 9 at great distances from the origin and which gives on the surface of the ellipsoid

$$u = \omega_2 z - \omega_3 y, \quad v = \omega_3 x - \omega_1 z, \quad w = \omega_1 y - \omega_2 x, \tag{12}$$

that is to say at the surface of the ellipsoid the fluid moves with the velocity of the ellipsoid, i.e. the relative velocity between the fluid and the surface of the particle is zero at any point of the surface. Jeffery calculates the values of u, v, w in terms of known parameters at any point and from these he calculates the stresses on the surface of the ellipsoid. From these he computes the components of force per unit area acting on the surface of the ellipsoid and the resultant couples (i.e. the torques) along each one of the axes x,y,z i.e. L_x, L_y, and L_z respectively.

Finally, Jeffery assumes that if the particle is subject to no forces except those exerted by the fluid upon its surface, then in the slow motions to which his assumptions have already restricted us, the resultant couple on the particle must vanish at every instant. This is a special case of what is also known as Stokes' flow and is equivalent to saying that at low particle Reynolds numbers, the net torque is zero, i.e. the angular acceleration is zero. This leads him to an expression for the steady-state components of angular velocity in the following specific case:

Take axes x', y', z' fixed in direction and let the components of the fluid velocity in the undisturbed motion (i.e. far from the particle) be u_0', v_0' and w_0', parallel to these axes. Consider the laminar motion given by $u_0' = v_0' = 0$ and $w_0' = Gy'$ where G is the constant velocity gradient in the + y' direction. This is recognized immediately as Couette flow, the flow which would occur when the gap between two infinite parallel surfaces is filled with fluid and one surface is made to move while the other remains stationary. This situation can be reproduced experimentally by two concentric cylinders separated by a gap of dimensions small compared to the length and diameter of the cylinders. The velocity of rotation, of course, will have to remain below the critical value at which organized or random turbulence (Taylor flow (21,22)) begins -- the motion is strictly laminar. The velocity w_0' at any point 0 is wholly in the z'-direction, while the velocity gradient is in the y' direction which coincides with the radius of the concentric cylinders. The outer cylinder is rotating so that the positive y' direction is the direction of increasing velocity. Figures 1, 2 and 3 show the geometry of the two systems of coordinates x,y,z and x',y',z' with respect to the concentric cylinder and the particle.

Since use is made in this study of Jeffery's results, his coordinate notation is adopted throughout. Thus his three Euler angles θ, φ, and ψ, connecting the systems x,y,z and x',y',z', are the angles between the axes x and x', the planes $x'y'$ and $x'x$ and the planes $x'x$ and xy respectively. As shown in Appendix A these angles are produced from the initial fixed system x', y', z', first by rotation about x' counterclockwise by an angle φ to produce the system of orthogonal axes x', y'', z'', then by rotation about z'' counterclockwise by an angle θ to produce the system x, y''', z'' and finally by rotation about x counterclockwise by an angle ψ to produce the system x,y,z. Then the steady-state motion* due to hydrodynamic forces is described by

$$\dot{\theta} = G\left(\frac{a^2 - b^2}{a^2 + b^2}\right) \sin\theta \cos\theta \sin\varphi \cos\varphi = \dot{\theta}_H , \qquad (13)$$

and

$$\dot{\varphi} = \frac{G}{(a^2 + b^2)} (a^2 \cos^2\varphi + b^2 \sin^2\varphi) = \dot{\varphi}_H , \qquad (14)$$

where a is the semimajor axis and b the semiminor axis of the ellipsoid and subscript H indicates these are hydrodynamic components. These formulas of Jeffery for the rate of change of $\dot{\theta}$ and $\dot{\varphi}$ due to the hydrodynamic forces were used by A. Peterlin (17) in his theory for SBR and since Peterlin's theory has been repeatedly verified (vis. Cerf and Scheraga (1)), we may conclude that the validity of these formulas and therefore Jeffery's treatment of the hydrodynamic part of the problem is proven and his expressions for the hydrodynamic torques are correct.

---

*That is the motion resulting from setting the acceleration terms $\dot{\omega}_1$, $\dot{\omega}_2$, and $\dot{\omega}_3$ equal to zero.

However equations 13 and 14 are not sufficient to characterize the angular velocity of the particle when an electrostatic orienting field is also present. It is not immediately obvious whether the electrostatic components and the hydrodynamic components of $\dot{\varphi}$ and $\dot{\theta}$ are linearly independent and additive. Therefore the new values of $\dot{\varphi}$ and $\dot{\theta}$ must be derived taking into account both effects. The starting point for the derivation is the simple statement that the resultant torque on the ellipsoids is equal to the sum of the torque due to the hydrodynamic field plus the torque due to the electric field. The torque due to the electric field will first be decomposed into components L_{Ex}, L_{Ey} and L_{Ez}; these components will then be added to the hydrodynamic components L_{Hx}, L_{Hy} and L_{Hz} available from Jeffery's theory, and the sum will be set equal to zero (i.e. $\dot{\omega}_1 = \dot{\omega}_2 = \dot{\omega}_3 = 0$) to obtain the values of ω_1, ω_2 and ω_3. From these the values of $\dot{\theta}$ and $\dot{\varphi}$ will be obtained by a simple transformation and the vector $\vec{\omega}$ will be expressed in terms of θ and φ. This value will be inserted into equation 6 and a solution will be obtained for the distribution orientation function, $F(\varphi,\theta)$.

A. RECAPITULATION OF UNDERLYING ASSUMPTIONS.

It is appropriate at this stage to list the assumptions on which this theory is based.

1. The flow is a continuum.
2. The flow is laminar.
3. The flow is one-dimensional with a constant velocity gradient.
4. The inertia terms (or the accelerations) of the equations of

motion of the fluid or of the particles are negligible, i.e. this is a Stokes flow.

5. The system is a monodisperse suspension.
6. The particles are rigid ellipsoids of revolution with semi-major axis a and semi-minor axis b = c.
7. The particles have either a uniform dielectric constant or two principal dielectric constants along the axes a and b.
8. The system has reached a steady state.
9. The electric field is one-dimensional and uniform and perpendicular to the velocity vector or parallel to the velocity gradient.
10. The electric field induces a dipole on the particle which does not have a permanent dipole moment and is non-conducting in the interior.

B. EFFECT OF THE ELECTRIC TORQUE ACTING ON THE PARTICLE.

To determine the effect of the electric torque on the orientation of the particle it will first be necessary to find the components of the torque along the fixed axes x', y' and z', to convert these into components along x, y and z, and to express these in terms of φ, θ and ψ, to determine the new spins ω_1, ω_2, and ω_3 and to insert these into the diffusion equation.

<u>1. Components of the Electric Torque Along x', y' and z'.</u>

The two angles of interest in considering the torque acting on the particle due to the electric field are the angle α made by the principal axis x (or a) of the particle and the electric field and the angle δ'', measured counterclockwise, made by the resultant electric torque L_E and the +x' axis. The direction of the electric field of strength E is entirely along the y' axis. Therefore the torque L_E due to this field is entirely in the x'z' plane as shown in figure 4. In addition the torque L_E is perpendicular to the axis of rotational symmetry of the particle x, and lies in each of the four quadrants of the x'z' plane depending on the orientation of the particle in the x'y'z' frame (figs. 4a, 4b, 4c and 4d). The angle δ', which is the smallest angle made by the torque L_E and the x' axis, is equal to the angle δ made by the perpendicular AC from the axis x to the axis y' and the perpendicular to the y' axis BC contained in the y'z' plane (since their sides are mutually perpendicular). Then, as shown in Appendix B, the following relations hold:

$$\sin 2\alpha = 2 \sin\theta \cos\varphi \sqrt{\sin^2\theta \sin^2\varphi + \cos^2\theta}\ , \tag{15}$$

$$\delta = \delta', \tag{16}$$

$$\cos\delta = \frac{\sin\theta \sin\varphi}{\sqrt{\cos^2\theta + \sin^2\theta \sin^2\varphi}}\ , \tag{17}$$

and

$$\sin\delta = \frac{\cos\theta}{\sqrt{\cos^2\theta + \sin^2\theta \sin^2\varphi}}\ . \tag{18}$$

It may be seen from figures 4a, b, c and d that the four pairs of components $L_{Ex'}$ and $L_{Ez'}$ resulting from all the possible orientations of the particle, can be expressed quite readily in terms of δ", which is seen to be related to δ' in each instance. It should be noted that the torque L_E is always drawn perpendicular on the plane of α with a counterclockwise (right-handed screw) convention. The four possible

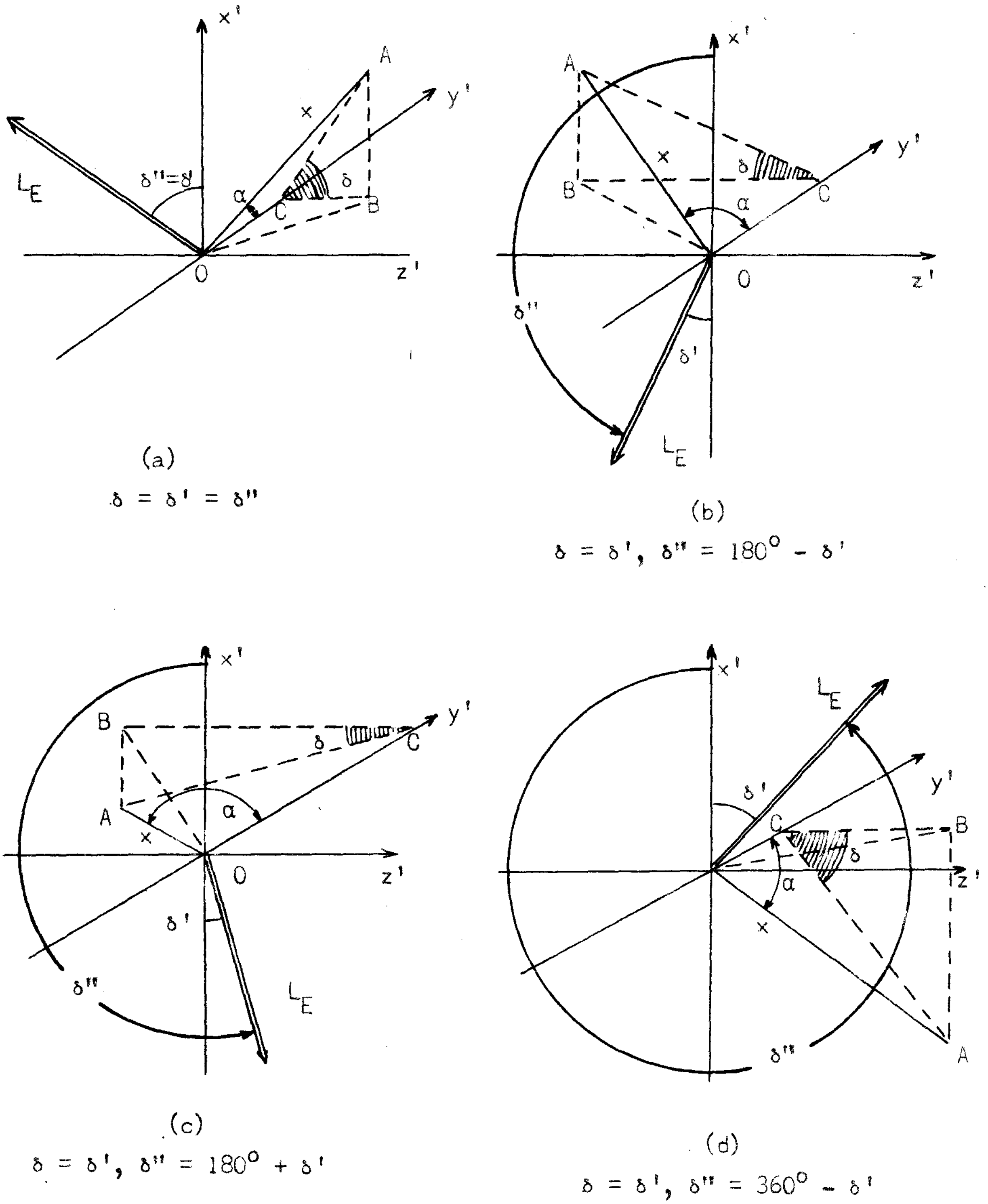

FIGURE 4

COORDINATE SYSTEM FOR DETERMINING COMPONENTS
OF ELECTRIC TORQUE ALONG x', y' and z'

pairs are shown in the following tabulation

Fig. 4a. $\delta = \delta' = \delta''$

$L_{Ex'} = L_E \cos \delta'$

$L_{Ez'} = - L_E \sin \delta'$

Fig. 4b. $\delta = \delta'$, $\delta'' = 180^\circ - \delta'$

$L_{Ex'} = - L_E \cos \delta'' = L_E \cos \delta'$

$L_{Ez'} = - L_E \sin \delta'' = - L_E \sin \delta'$

Fig. 4c. $\delta = \delta'$, $\delta'' = 180^\circ + \delta'$

$L_{Ex'} = - L_E \cos \delta'' = L_E \cos \delta'$

$L_{Ez'} = L_E \sin \delta'' = - L_E \sin \delta'$

Fig. 4d. $\delta = \delta'$, $\delta'' = 360^\circ - \delta'$

$L_{Ex'} = L_E \cos \delta'' = L_E \cos \delta'$

$L_{Ez'} = L_E \sin \delta'' = - L_E \sin \delta'$

It is obvious that in all cases

$$\left.\begin{aligned} L_{Ex'} &= L_E \cos \delta, \\ L_{Ey'} &= 0, \\ \text{and} \quad L_{Ez'} &= -L_E \sin \delta, \end{aligned}\right\} \qquad (19)$$

where, as shown in Appendix C,

$$L_E = BE^2 \sin 2\alpha. \qquad (20)$$

The quantity B is a constant given in Appendix C which contains the dielectric constant and the dimensions of the particle.

2. Components of the Electric Torque Along x, y and z, in Terms of φ, θ and ψ.

Inserting the value of L_E given by equations 15 and 20 in equations 19 and operating on it with the transformation matrix A of Appendix A, we obtain the components of the torque along x, y and z, namely

$$\left.\begin{aligned} L_{Ex} &= 0 \\ L_{Ey} &= -BE^2(2\sin\theta\cos\varphi)(\sin\varphi\cos\psi + \cos\theta\cos\varphi\sin\psi) \\ \text{and}\quad L_{Ez} &= BE^2(2\sin\theta\cos\varphi)(\sin\varphi\sin\psi - \cos\theta\cos\varphi\cos\psi) \end{aligned}\right\} \quad (21)$$

Note that $L_{Ex} = 0$ as one would suspect intuitively because of symmetry.

This concludes the determination of the components of the electric torque.

3. <u>New Spins ω_1, ω_2 and ω_3 Due to the Combined Electric and Hydrodynamic Torques.</u>

The hydrodynamic components of the torque along x, y and z axes, as derived by Jeffery, are

$$\left.\begin{aligned} L_{Hx} &= A_x\{2b^2(f_2 - \omega_1)\}, \\ L_{Hy} &= A_y\{(b^2 - a^2)g_1 + (b^2 + a^2)(g_2 - \omega_2)\}, \\ L_{Hz} &= A_z\{(a^2 - b^2)h_1 + (a^2 + b^2)(h_2 - \omega_3)\}. \end{aligned}\right\} \quad (22)$$

The symbols A_x, A_y, A_z, g_1, h_1, f_2, g_2 and h_2 are defined in Appendix D. The components of the combined torques are given, in the steady state, by

$$\left.\begin{aligned} L_x &= L_{Hx} + L_{Ex} = 0 \\ L_y &= L_{Hy} + L_{Ey} = 0 \\ L_z &= L_{Hz} + L_{Ez} = 0 \end{aligned}\right\} \quad (23)$$

Inserting equations 21 and 22 into equation 23 and solving for ω_2 and ω_3 (note that ω_1 is not required since ψ is not required because ψ is arbitrary), we obtain

$$\omega_2 = \frac{A_y[(b^2 - a^2)g_1 + (b^2 + a^2)g_2] - BE^2(2\sin\theta\cos\varphi)(\sin\varphi\cos\psi + \cos\theta\cos\varphi\cos\psi)}{A_y(b^2 + a^2)}$$

$$\equiv \dot{\theta}\sin\psi - \dot{\varphi}\sin\theta\cos\psi, \tag{24}$$

$$\omega_3 = \frac{A_z[(a^2 - b^2)h_1 + (a^2 + b^2)h_2] + BE^2(2\sin\theta\cos\varphi)(\sin\varphi\cos\psi - \cos\theta\cos\varphi\cos\psi)}{A_z(a^2 + b^2)}$$

$$\equiv \dot{\theta}\cos\psi + \dot{\varphi}\sin\theta\sin\psi.$$

4. New Spins $\dot{\varphi}$ and $\dot{\theta}$ Due to the Combined Electric and Hydrodynamic Torques.

Inserting the values for g_1, g_2, h_1 and h_2 from Appendix D into equations 24 and solving for $\dot{\varphi}$ and $\dot{\theta}$, we obtain, after considerable simplification,

$$\dot{\varphi} = \frac{G}{(a^2+b^2)}(a^2\cos^2\varphi + b^2\sin^2\varphi) + \frac{BE^2}{(a^2+b^2)} \cdot \frac{1}{A_y} \circ 2\cos\varphi\sin\varphi$$

and

$$\dot{\theta} = \frac{G(a^2-b^2)}{4(a^2+b^2)}\sin 2\theta\sin 2\varphi - \frac{BE^2}{(a^2+b^2)} \cdot \frac{1}{A_y} \cdot \sin 2\theta\cos^2\varphi \tag{25}$$

where $A_y = A_z$ (since $b = c$) is defined in Appendix D.

Recognizing the first terms in the right-hand side of equations 25 for the hydrodynamic contributions to $\dot{\varphi}$ and $\dot{\theta}$, we may write

$$\dot{\varphi} = \dot{\varphi}_H + \dot{\varphi}_E$$

and

$$\dot{\theta} = \dot{\theta}_H + \dot{\theta}_E \tag{26}$$

where

$$\left.\begin{aligned} \dot{\varphi}_E &= \frac{1}{A_y} \cdot \frac{BE^2}{a^2 + b^2} \cdot \sin 2\varphi \\ \text{and} \qquad \dot{\theta}_E &= -\frac{1}{A_y} \cdot \frac{BE^2}{a^2 + b^2} \cdot \sin 2\theta \cos^2\varphi . \end{aligned}\right\} \quad (27)$$

Note that ψ does not appear in the expressions for $\mathring{\varphi}$ and $\dot{\theta}$, as one would suspect from the symmetry of the particles.

C. SPECIAL CASE OF THE GENERAL ORIENTATION DIFFUSION EQUATION FOR RIGID COLLOIDAL PARTICLES IN COUETTE FLOW WITH AN ELECTRIC FIELD NORMAL TO THE VELOCITY.

In the spherical coordinate system with its origin at the center of the particle of unit radius and polar angles φ and θ (identical with the Euler angles), the angular flux $\vec{\omega}$ of the particle due to the external orienting fields is given by

$$\vec{\omega} = \frac{d\vec{\Omega}}{dt} = \frac{d\theta}{dt}\,\vec{\theta}_1 + \sin\theta\,\frac{d\varphi}{dt}\,\vec{\varphi}_1 \qquad (28)$$

where $d\vec{\Omega}$ is the angle through which the particle turns and consists of the components $d\theta$ and $\sin\theta\, d\varphi$ in the $\vec{\theta}_1$ and $\vec{\varphi}_1$ dimensions respectively.

The term div $F(\vec{\omega})$ in the steady-state orientation diffusion equation, equation 6, now becomes

$$\nabla\cdot F\vec{\omega} = \frac{1}{\sin\theta}\left[F\dot{\theta}\cos\theta + F\frac{\partial\dot{\theta}}{\partial\theta}\sin\theta + \dot{\theta}\frac{\partial F}{\partial\theta}\sin\theta + \sin\theta\dot{\varphi}\frac{\partial F}{\partial\varphi} + F\sin\theta\frac{\partial\dot{\varphi}}{\partial\varphi}\right] \qquad (29)$$

To simplify the computation of this term construct the right triangle shown in figure 5 and set $M = A \sin 2\lambda$ and $2K = A \cos 2\lambda$ where $K = \frac{1}{4}\,G\left(\frac{a^2 - b^2}{a^2 + b^2}\right) = \frac{1}{4}\,GR$ and $M = \frac{1}{A_y}\left(\frac{BE^2}{a^2 + b^2}\right)$. Then we obtain

$$\dot{\varphi} = A[\cos(2\varphi - 2\lambda) + \frac{\cos 2\lambda}{R}]$$

and (30)

$$\dot{\theta} = \frac{A}{2}\sin 2\theta[\sin(2\varphi - 2\lambda) - \sin 2\lambda].$$

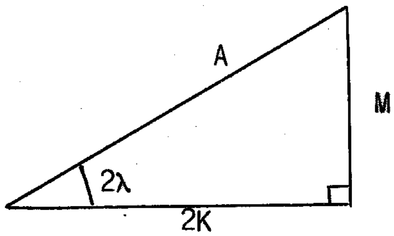

FIGURE 5
TRANSFORMATION OF COORDINATES

Now let $2\varphi - 2\lambda = 2\gamma$. Note that 2λ is a constant which depends on the magnitude of the electric field E, the velocity gradient G, the dimensions and the dielectric constant of the particle. Then we obtain

$$\frac{\partial F}{\partial \varphi} = \frac{\partial F}{\partial \gamma}\ , \quad \frac{\partial^2 F}{\partial \varphi^2} = \frac{\partial^2 F}{\partial \gamma^2} \ \text{and} \ \frac{\partial \dot{\varphi}}{\partial \varphi} = \frac{\partial \dot{\varphi}}{\partial \gamma}\ , \tag{31}$$

and equation 29 becomes

$$\nabla \cdot F\vec{\omega} = \frac{A}{\sin\theta}[(-3\sin^3\theta \sin 2\gamma - \sin\theta(3\cos^2\theta - 1)\sin 2\lambda)F$$

$$+ \frac{1}{2}\sin\theta \sin 2\theta(\sin 2\gamma - \sin 2\lambda)\frac{\partial F}{\partial \theta}$$

$$+ \sin\theta(\cos 2\gamma + \frac{1}{R}\cos 2\lambda)\frac{\partial F}{\partial \gamma}]. \tag{32}$$

Note that when E = 0, the quantities M and sin 2λ vanish while cos $2\lambda = 1$, and we obtain A = 2K and $\gamma = \varphi$. Then equation 32 is identical with the equivalent term $\nabla \cdot F\vec{\omega}$ in Peterlin's theory (17).

Carrying through all these transformations to the left-hand side of equation 6, we obtain

$$D\nabla^2 F = D\left\{\frac{1}{\sin^2\theta}\frac{\partial^2 F}{\partial \gamma^2} + \frac{\cos\theta}{\sin\theta}\frac{\partial F}{\partial \theta} + \frac{\partial^2 F}{\partial \theta^2}\right\}. \tag{33}$$

When E = 0 equation 23 also becomes identical with the equivalent term $D\nabla^2 F$ in Peterlin's theory.

Equations 6, 32 and 33 now give the special case of the orientational diffusion equation for rigid colloidal particles in Couette flow with an electric field normal to the velocity.

D. SOLUTION OF THE ORIENTATIONAL DIFFUSION EQUATION FOR RIGID COLLOIDAL PARTICLES IN COUETTE FLOW WITH AN ELECTRIC FIELD NORMAL TO THE VELOCITY.

The form of equation 6 which applies to our problem can now be written

$$\nabla^2 F = \frac{A}{D} \{-(3 \sin^2\theta \sin 2\gamma + [3 \cos^2\theta - 1] \sin 2\lambda)F$$

$$+ \frac{1}{2} \sin 2\theta \ (\sin 2\gamma - \sin 2\lambda) \frac{\partial F}{\partial \theta}$$

$$+ (\cos 2\gamma + \frac{1}{R} \cos 2\lambda) \frac{\partial F}{\partial \gamma} \}, \qquad (35)$$

where

$$A = R\sqrt{\frac{1}{4} G^2 + \frac{B^2 E^4}{A_y{}^2 (a^2 - b^2)^2}} \,. \qquad (36)$$

We recognize equation 35 as a linear partial differential equation with transcendental coefficients. A certain symmetry is expected to prevail on physical grounds (e.g. $F(\varphi,\theta) = F(\varphi + \pi, \theta + \pi)$) and the orientation distribution function should be a sphere of unit radius with a variable population density on its surface. In addition, the quantity A/D is usually less than unity. Thus for tobacco-mosaic virus $R \doteq 1$, $D \doteq 530 \text{ sec}^{-1}$; for thymonucleic acid $D \doteq 400 - 1150 \text{ sec}^{-1}$, $R < 1.0$; and for vanadium pentoxide $D \doteq 180$, $R < 1.0$. Since usually turbulence sets in for $G \doteq 1000 \text{ sec}^{-1}$ most SBR measurements are made with $G \doteq 100$ or less. The magnitude of E on the other hand should remain small to avoid electrophoresis so that $BE^2/A_y(a^2 - b^2)$ remains usually below 50 sec^{-1}. Thus, usually, $A/D \ll 70/100 < 1.0$. Therefore it appears that the function F may be expressed as a power series in A. In most applications this series converges fairly rapidly.

Letting

$$\beta = \frac{A}{D}, \tag{37}$$

the required series becomes

$$F = \sum_{j=0}^{\infty} \beta^j F_j \tag{38}$$

where each F_j satisfies the inhomogeneous equation

$$\begin{aligned} \nabla^2 F_j &= -(3 \sin^2\theta \sin 2\gamma + [3 \cos^2\theta - 1] \sin 2\gamma) F_{j-1} \\ &+ \frac{1}{2} \sin 2\theta \, (\sin 2\gamma - \sin 2\lambda) \frac{\partial F_{j-1}}{\partial \theta} \\ &+ (\cos 2\gamma + \frac{1}{R} \cos 2\lambda) \frac{\partial F_{j-1}}{\partial \gamma}. \end{aligned} \tag{39}$$

Because of the spherical characteristics of F, each F_j may be expressed in terms of a series of spherical harmonics as:

$$F_j = \frac{1}{2} \sum_{n=0}^{\infty} a_{n0,j} P_{2n} + \sum_{n=1}^{\infty} \sum_{m=1}^{n} (a_{nm,j} \cos 2m\gamma + b_{nm,j} \sin 2m\gamma) P_{2n}^{2m}. \tag{40}$$

The computation of the terms F_0, F_1 etc. is given in Appendix E. The procedure we follow in order to determine the coefficients $a_{n0,j}$, $a_{nm,j}$ and $b_{nm,j}$ is as follows: Express each of the terms $3 \sin^2\theta \sin 2\gamma$, $(3 \cos^2\theta - 1)\sin 2\gamma$, $\frac{1}{2} \sin 2\theta(\sin 2\gamma - \sin 2\lambda)$, $\cos 2\gamma + \frac{1}{R} \cos 2\lambda$ of equation 39 in terms of spherical harmonics of the first kind $P_{2n}(x)$

(Legendre polynomials) or associated spherical harmonics of the first kind $P_{2n}^{2m}(x)$ (Legendre associated functions).* Also express F_{j-1}, $\frac{\partial F_{j-1}}{\partial \theta}$ and $\frac{\partial F_{j-1}}{\partial \gamma}$ in terms of Legendre polynomials or Legendre associated functions. Then substitute these terms with the appropriate equivalent polynomials or functions on each side of equation 39 and carry out the multiplications involved, grouping the terms which include same powers of x and at the same time like trigonometric factors sin $2m\gamma$ or cos $2m\gamma$. Then equate the coefficients of like terms on each side, i.e. terms of the type x^i, $x^i \sin 2m\gamma$ or $x^i \cos 2m\gamma$, $(i = 0,1,2,...;\ m = 1,2,...)$. Then solve the resulting system of simultaneous equations for the coefficients $a_{n0,j}$, $a_{nm,j}$, $b_{nm,j}$. It should be noted that this method becomes possible because the products of spherical harmonics involved all turn out to be finite polynomials. Thus the general term will include the products $P_2^2 P_{2n} = 3(1-x^2)P_{2n}$; $P_2^2 P_{2n}^{2m} = 3(1-x^2)P_{2n}^{2m}$; $P_2 P_{2n} = \frac{1}{2}(3x^2-1)P_{2n}$; $P_2 P_{2n}^{2m} = \frac{1}{2}(3x^2-1)P_{2n}^{2m}$; (where P_{2n}^{2m} is a finite polynomial); $P_2^1 P_{2n}^1 = 3(1-x^2)^{1/2} x \cdot (1-x^2)^{1/2} \cdot$[a finite polynomial]; $\cot\theta\ P_2^1 P_{2n}^{2m} = 3x(1-x^2)^{-1/2}(1-x^2)^{1/2} \cdot P_{2n}^{2m}$; $-P_2^1 P_{2n}^{2m+1} = -3x(1-x^2)^{1/2}(1-x^2)^{1/2} \cdot$[a finite polynomial], for $m < n$ and $-P_2^1 P_{2n}^{2m+1} = 0$ for $m = n$. These tedious but straightforward steps outlined above and leading to the values of the general coefficients were not carried out and only the coefficients of the first three terms were determined.

Finally it will be seen that all coefficients can be expressed in terms of the leading coefficient, $a_{00,0}$, whose value can be found by normalization i.e. by setting the integral of F over the entire solid angle

---

*It is convenient to use the notation of Jahnke and Emde (Tables of Functions, Dover Publications, New York, Fourth Ediction, 1945) and define $P_n(x) = P(\cos\theta)$ and $P_n^n(x) = P_n^n(\cos\theta)$ so that $P_1(x) = \cos\theta = x$ and $P_1^1(x) = \sin\theta = (1 - x^2)^{1/2}$.

(over the surface of the unit sphere) equal to unity. Thus

$$\int_{\Omega} F \, d\Omega = \int_0^{2\pi} \int_0^{\pi} F \sin\theta \, d\theta \, d\varphi = 1 \tag{41}$$

Because of the orthogonality of the terms of F, only F_0 survives the integration yielding $a_{00,0} = \frac{1}{2\pi}$.

The first three terms were determined by following the same procedure outlined above. The details of that computation are given in Appendix E. The series F then becomes

$$F = \frac{1}{4\pi} + \beta[\tfrac{1}{2} a_{10,1}P_2 + (a_{11,1}\cos 2\gamma + b_{11,1}\sin 2\gamma)P_2^2]$$

$$+ \beta^2[\tfrac{1}{2} a_{10,2}P_2 + (a_{11,2}\cos 2\gamma + b_{11,2}\sin 2\gamma)P_2^2 + \tfrac{1}{2} a_{20,2}P_4$$

$$+ (a_{21,2}\cos 2\gamma + b_{21,2}\sin 2\gamma)P_4^2 + (a_{22,2}\cos 4\gamma + b_{22,2}\sin 4\gamma)P_4^4] + .. \tag{42}$$

The values of the coefficients $a_{10,1}$, $a_{11,1}$, $a_{10,2}$, $a_{11,2}$, $b_{11,2}$, $a_{20,2}$, $a_{21,2}$, $b_{21,2}$, $a_{22,2}$, and $b_{22,2}$ and the Legendre polynomials P_2, P_4 and associated functions P_2^2, P_4^2, P_4^4 (which happen to be polynomials in this case) are also given in Appendix E.

The following general rules were found to hold for the coefficients of equations 38 to 40:

1. All terms with negative indexes are zero.
2. All P_{2n}^{2m+1} are zero when $m = n$.
3. $a_{nm,0} = 0$ and $a_{00,j} = 0$ except $a_{00,0} = \frac{1}{2\pi}$.
4. $b_{nm,0} = b_{n0,j} = b_{0m,j} = 0$.
5. If $n > j$ or if $m > j$, $a_{nm,j} = 0$.
6. Terms with $m > n$ are excluded.

Some of these rules were also found to hold in the investigation of SBR by Scheraga, Edsall and Gadd (18). It should be pointed out that not all the coefficients are required for the SBR problem, but, as was shown by Peterlin and Stuart only the $b_{11,j}$ and $a_{11,j}$ terms are retained. It is difficult to say without further analysis which terms will be retained when the electrohydrodynamically oriented system interacts with a polarized beam of light to give double refraction by a combination of the Kerr and Maxwell effects (i.e. electrostreaming birefringence, ESBR). In principle, however the evaluation of the angle of extinction and the birefringence can be carried out by the method of Peterlin and Stuart (11). That computation is beyond the scope of this study but will be carried out at a future date.

III. CONCLUSIONS

The orientation distribution function for rigid colloidal particles in Couette flow with an electric field normal to the velocity was derived. It contains terms with coefficients involving the factors

$$\beta = \frac{1}{D}\sqrt{M^2 + 4K^2} = \frac{A}{D}$$

$$\beta \sin 2\lambda = \frac{M}{D}$$

$$\beta \cos 2\lambda = \frac{2K}{D}$$

$$(\beta^2 \cdot b_{11,2} \sin 2\gamma) \propto (\beta^2 \sin 2\lambda \sin 2\gamma) = \beta^2 \sin 2\lambda \sin (2\varphi - 2\lambda)$$

$$= \beta^2 \sin 2\lambda (\sin 2\varphi \cos 2\lambda - \cos 2\varphi \sin 2\lambda)$$

$$= \sin 2\varphi \cdot \beta^2 \cdot \sin 2\lambda \cos 2\lambda - \cos 2\varphi \cdot \beta^2 \sin^2 2\lambda$$

$$= \frac{2MK}{D^2} \cdot \sin 2\varphi - \frac{M^2}{D^2} \cos 2\varphi ,$$

$$(\beta^2 \cdot a_{11,2} \cos 2\gamma) \propto \frac{2MK}{D^2} \cdot \sin 2\varphi + \frac{4K^2}{D^2} \cdot \cos 2\varphi, \text{ etc.}$$

These clearly contain products MK of the electric field and the velocity gradient as well as functions of the squares of the electric field and the velocity gradient. Therefore the addition of the two effects is non-linear and one would expect that the simultaneous application of the two effects will yield new information independently. For example if the size and shape of the particle is found by SBR and the rotary diffusion coefficient, D, is found by EBR (the Kerr effect) then the dielectric constant can be found by ESBR.

The orientation-distribution function derived here can be used to determine the angle of extinction, χ, and the birefringence, Δn, of colloidal suspensions subjected to the simultaneous application of electric and hydrodynamic fields. Both these quantities will contain products of the terms M and K as well as the sum of their squares and the incomplete expressions of Tolstoi, equations 1 and 2, are of very limited value. The technique of measuring χ and Δn may be improved by carrying out experiments at a constant velocity gradient with a variable electric field.

Since the viscosity of a suspension or solution depends on the distribution of orientations of the suspended or solute particles (v. Peterlin (17)), it appears that the viscosity is dependent on the electrostatic field. The orientation-distribution function for ESBR derived here can also be used to study that dependence.

REFERENCES

1. R. Cerf and H. A. Scheraga, Chem. Rev., 51, 185 (1952).

2. R. H. Humphry, Proc. Roy. Soc. (London) 35, 217 (1923).

3. H. Wayland, J. App. Phys., 26, 1197 (1955).

4. J. W. Prados and F. N. Peebles, The Analysis of Two-Dimensional Laminar Flow Utilizing a Doubly Refracting Liquid, Final Report NONR-811(04), Univ. of Tennessee, June (1957).

5. F. N. Peebles, J. W. Prados, E. H. Honeycutt, A Study of Laminar Flow Phenomena Utilizing a Doubly Refracting Liquid, Progress Report 1, NONR-811(04), Univ. of Tennessee, July (1954).

6. H. Benoit, Compt. rend., 228, 1716 (1949).

7. H. Benoit, Thesis, University of Strassbourg, Contribution a l'Etude de l'Effet Kerr Presente par les Solutions Diluees de Macromolecules Rigides, Masson et Cie, Paris (1950).

8. C. T. O'Konski and B. H. Zimm, Science, 111, 113 (1950).

9. C. T. O'Konski and A. J. Haltner, J. Am. Chem. Soc., 78, 3604 (1956).

10. N. A. Tolstoi, Doklady Akad. Nauk. S.S.S.R., 59, 1563 (1948).

11. A. Peterlin and H. A. Stuart, Z. Physik, 112, 1, 129 (1939).

12. A. Peterlin and H. A. Stuart, Hand-und Jahrbuch der chemischen Physik, Bd. VIII, Abt. 1B, Becker and Erler, Leipzig (1943).

13. C. V. Raman and K. S. Krishnan, Proc. Roy. Soc. (London) 117A, 589 (1928).

14. C. J. Sadron, J. phys. radium [7] 7, 263 (1936).

15. C. J. Sadron, J. phys. radium [7], 8, 481 (1937).

16. F. Perrin, J. phys. radium [7], 5, 497 (1934).

17. A. Peterlin, Z. Physik 111, 232 (1938).

18. H. A. Scheraga, J. T. Edsall and J. O. Gadd Jr., J. Chem. Phys. 19, 1101 (1951).

19. O. Snellman and Y. Björnstahl, Kolloid-Beihefte 52, 403 (1941).

20. G. B. Jeffery, Proc. Roy. Soc. (London), A102, 161 (1922-23).

21. G. I. Taylor, Trans. Roy. Soc. (London) A223, 289 (1923).

22. G. I. Taylor, Proc. Roy. Soc. (London) A157, 565 (1936).

23. W. R. Smythe, Static and Dynamic Electricity, 2nd Edition, 2nd Impression, McGraw-Hill Book Co., Inc., pp. 208-209 (1950).

24. E. A. Hauser, Colloidal Phenomena, 1st Edition, 5th Impression, McGraw-Hill Book Co., Inc., pp. 89-113 (1939).

25. C. T. O'Konski and A. J. Haltner, J. Am. Chem. Soc., 79, 5634 (1957).

26. J. T. Edsall, A. Rich and M. Goldstein, Rev. Sci. Instruments, 23, 685 (1952).

APPENDIX A

COORDINATE SYSTEMS AND TRANSFORMATIONS OF THE ORIENTATION PROBLEM

Use is made in this study of some of the results of Jeffery (20) and therefore his coordinate system is adopted in describing the orientation of the general particle. Thus axes x', y', z' are fixed in direction with x' along the axis of the concentric cylinders, y' along the direction of the velocity gradient (i.e. along the radius from the inner to the outer cylinder when the outer is rotating) and z' along the direction of the flow velocity (see figures 1, 2 and 3 of the text). The axes of the ellipsoid (fixed in the ellipsoid and rotating with it) are x, y and z, with the semi-major axis laid out on x. Jeffery gives the direction cosines of the axes of the ellipsoid (x,y,z) referred to the axes x', y', z' with values $(\ell_1, m_1, n_1)(\ell_2, m_2, n_2)$ and (ℓ_3, m_3, n_3) respectively. Then he introduces the three Euler angles, θ, the angle between the axes x and x', φ, the angle between the planes $x'y'$ and $x'x$, and ψ, the angle between the planes of $x'x$ and xy. As may be seen from figures 1, 2 and 3 of this Appendix, the coordinate system x,y,z may be formed from the system x', y', z' by the following sequence of rotations:

First rotate about x' counterclockwise by an angle φ to produce the system x', y'', z''. This transformation is represented by the matrix

$$D = \begin{pmatrix} 1 & 0 & 0 \\ 0 & \cos\varphi & \sin\varphi \\ 0 & -\sin\varphi & \cos\varphi \end{pmatrix} \qquad (1\text{-}A)$$

Then rotate about z'' counterclockwise by an angle θ to produce x, y''', z''. Note that now x is contained in the plane of x', y'', y'''. This transfor-

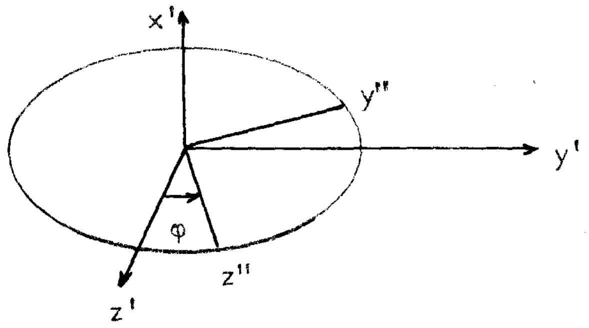

FIGURE 1, APPENDIX A

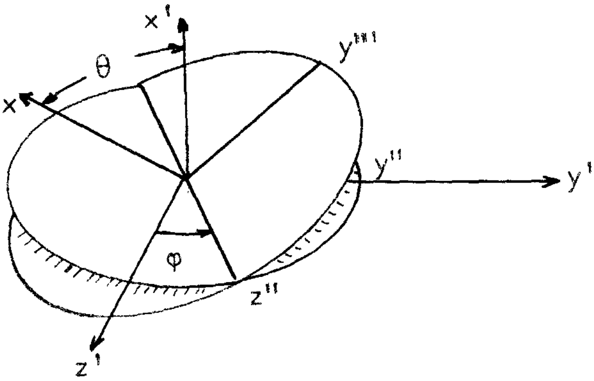

FIGURE 2, APPENDIX A

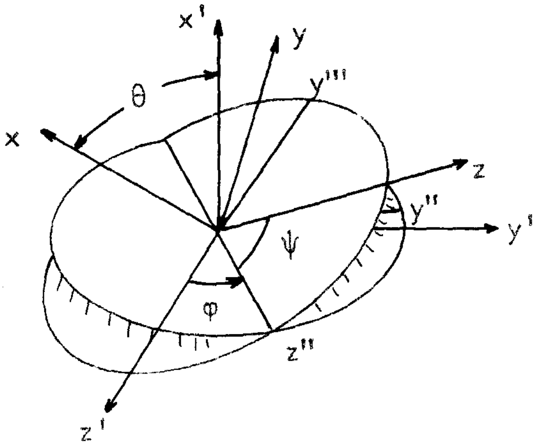

FIGURE 3, APPENDIX A

EULER ANGLES OF PARTICLES AND TRANSFORMATION OF AXES mation is represented by the matrix

$$C = \begin{pmatrix} \cos\theta & \sin\theta & 0 \\ -\sin\theta & \cos\theta & 0 \\ 0 & 0 & 1 \end{pmatrix} \tag{2-A}$$

Finally rotate about x counterclockwise by the angle ψ to produce the system x,y,z. This transformation is represented by the matrix

$$B = \begin{pmatrix} 1 & 0 & 0 \\ 0 & \cos\psi & \sin\psi \\ 0 & -\sin\psi & \cos\psi \end{pmatrix} \tag{3-A}$$

Finally the complete transformation from x',y',z' to x,y,z is given by the product matrix A,

$$A = BCD, \tag{4-A}$$

$$A = \begin{pmatrix} \cos\theta & \sin\theta\cos\varphi & \sin\varphi\sin\theta \\ -\sin\theta\cos\psi & \cos\varphi\cos\psi\cos\theta - \sin\psi\sin\varphi & \sin\varphi\cos\psi\cos\theta + \sin\psi\cos\varphi \\ \sin\theta\sin\psi & -\sin\psi\cos\theta\cos\varphi - \sin\varphi\cos\psi & -\sin\varphi\sin\psi\cos\theta + \cos\psi\cos\varphi \end{pmatrix} \tag{5-A}$$

This corresponds to Jeffery's matrix

$$\begin{pmatrix} \ell_1 & m_1 & n_1 \\ \ell_2 & m_2 & n_2 \\ \ell_3 & m_3 & n_3 \end{pmatrix} \tag{6-A}$$

for the cosines of the angles

$$\hat{x}x', \quad \hat{x}y', \quad \hat{x}z'$$
$$\hat{y}x', \quad \hat{y}y', \quad \hat{y}z' \qquad (7\text{-}A)$$
$$\hat{z}x', \quad \hat{z}y', \quad \hat{z}z'$$

Using the matrix A we can transform any vector given in coordinates x', y', z' into a vector in coordinates x, y, z. Thus equations 21 of the text are derived by the operation

$$A \begin{pmatrix} L_{Ex'} \\ L_{Ey'} \\ L_{Ez'} \end{pmatrix} = \begin{pmatrix} L_{Ex} \\ L_{Ey} \\ L_{Ez} \end{pmatrix} \qquad (8\text{-}A)$$

It should be noted here that the angles φ, θ are identical with the normal spherical coordinates of a system with volume element

$$d\Omega = \sin\theta \, d\theta \, d\varphi \qquad (9\text{-}A)$$

Therefore the operators ∇^2 and div will be written directly in spherical coordinates with $r = 1$.

APPENDIX B

COMPONENTS OF THE ELECTROSTATIC TORQUE EXPRESSED IN TERMS OF THE EULER ANGLES

Of interest in this discussion are the angles α and δ'' between the axis x of the particle and the electric field and between the axis x' of the fixed frame and the electrostatic torque L_E (measured counterclockwise) respectively (see figures 4a, b, c and d of the text). It should be noted that L_E lies entirely on the plane of x'z' under all possible orientations of the particle (as long as the electric field is along the axis y').

Referring to figure 4a of the text notice that ABC, ACO, BCO and ABO are right triangles and the angle COB is φ. Then

$$AB = OA \sin (90^\circ - \theta) = OA \cos \theta,$$

$$OB = OA \cos (90^\circ - \theta) = OA \sin \theta,$$

$$OC = OB \cos \varphi$$

and therefore

$$OC = OA \sin \theta \cos \varphi = OA \cos \alpha.$$

In addition

$$CB = OB \sin \varphi$$

$$OB = OA \sin \theta$$

and therefore

$$CB = OA \sin \theta \sin \varphi.$$

Finally, since

$$(AC) = \sqrt{(AB)^2 + (BC)^2} = OA \sin \alpha$$

we obtain

$$\sin 2\alpha = 2 \sin \alpha \cos \alpha = 2 \sin \theta \cos \varphi \sqrt{\sin^2\theta \sin^2\varphi + \cos^2\theta} \quad (1\text{-B})$$

Again referring to figure 4a of the text, notice that

1. L_E is wholly on $x'z'$ plane since $L_E \perp E$.
2. Plane ACB $\parallel$ $x'z'$ and line AB $\parallel$ x'.
3. Therefore $L_E \parallel$ plane ACB.
4. In addition, $L_E \perp x$, since L_E is normal on xy' plane which contains the angle α between axes x and y'.

We may now prove that $\delta = \delta'$ as follows:*

5. CB $\perp$ $0x'$, since $x' \perp z'$ and $z' \parallel$ CB.
6. $L_E \perp$ AC, since AC is contained in plane xy'.
7. Therefore $L_E \perp$ AC.
8. Then $\delta = \delta'$ since their sides are mutually perpendicular and lie on parallel planes.

Observe now that

$$AB = 0A \cos \theta,$$

$$BC = AC \cos \delta,$$

$$BC = 0B \sin \varphi,$$

$$0B = 0A \sin \theta,$$

and therefore

$$BC = 0A \sin \theta \sin \varphi = AC \cos \delta.$$

Hence

$$\cos \delta = \frac{BC}{AC} = \frac{0A \sin \theta \sin \varphi}{\sqrt{(AB)^2 + (BC)^2}} = \frac{\sin \theta \sin \varphi}{\sqrt{\sin^2\theta \sin^2\varphi + \cos^2\theta}} \quad (2\text{-B})$$

---

*The angle δ' is the smallest angle made by the x' axis and L_E.

Finally,

$$AB = AC \sin \delta = OA \cos \theta$$

and therefore

$$\sin \delta = \frac{AB}{AC} = \frac{OA \cos \theta}{\sqrt{(AB)^2 + (BC)^2}} = \frac{\cos \theta}{\sqrt{\sin^2\theta \sin^2\varphi + \cos^2\theta}} \quad . \qquad (3\text{-}B)$$

APPENDIX C

ELECTROSTATIC TORQUE L_E ACTING ON A PROLATE SPHEROID

It may be shown that if a dielectric prolate spheroid (ellipsoid of revolution shaped like a cigar) with a relative capacitivity K (dielectric constant) is placed in an electric field E, its axis of revolution x making an angle α with the field, the torque acting on it is

$$L_E = \frac{2}{3}\pi e_w (K - 1) b^2 a E (E_1 - E_2) \sin 2\alpha. \qquad (1\text{-}C)$$

Here $K = \varepsilon/\varepsilon_w$ where ε and ε_w are the values of the capacitivity, dielectric constant or permittivity of the particle and of water, respectively, a is the semi-major axis, b is the semi-minor axis and E_1 and E_2 are the resultant field inside the particle when x is normal and when x is parallel to the field, respectively, given by

$$E_1 = - \frac{E}{\{(K - 1)s[(1 - s^2)\coth^{-1}s + s] - K\}} \qquad (2\text{-}C)$$

$$E_2 = \frac{2E}{\{2 + (K - 1)s[(1 - s^2)\coth^{-1}s + s\}} \qquad (3\text{-}C)$$

where

$$s = a(a^2 - b^2)^{-1/2}. \qquad (4\text{-}C)$$

Therefore

$$L_E = BE^2 \sin 2\alpha \qquad (5\text{-}C)$$

where

$$B = -\frac{2}{3}\pi\varepsilon_w (K - 1) b^2 a \left(\frac{1}{S_0 - K} + \frac{2}{2 + S_0}\right), \qquad (6\text{-}C)$$

and

$$S_0 = (K - 1)s[(1 - s^2) \coth^{-1} s + s]. \qquad (7\text{-}C)$$

These formulas are also given by Smythe (23). The dielectric constant of the particle may be adjusted to account for the Gouy-Freundlich (24) effect. The anomalous behavior of the dielectric constant of the particle was recently studied by O'Konski and Haltner (25).

APPENDIX D

DEFINITIONS OF SYMBOLS USED IN EXPRESSIONS FOR HYDRODYNAMIC TORQUES

According to Jeffery (20) and using his definitions (equation 6-A),

$$\left.\begin{aligned} f_1 &= \tfrac{1}{2}G(m_2n_3 + m_3n_2), & f_2 &= \tfrac{1}{2}G(m_2n_3 - m_3n_2), \\ g_1 &= \tfrac{1}{2}G(m_3n_1 + m_1n_3), & g_2 &= \tfrac{1}{2}G(m_3n_1 - m_1n_3), \\ h_1 &= \tfrac{1}{2}G(m_1n_2 + m_2n_1), & h_2 &= \tfrac{1}{2}G(m_1n_2 - m_2n_1), \end{aligned}\right\} \quad (1\text{-D})$$

while the spins $\omega_1, \omega_2, \omega_3$ can be written in terms of $\dot{\varphi}$, $\dot{\psi}$, and $\dot{\theta}$ as follows

$$\left.\begin{aligned} \omega_1 &\equiv \dot{\varphi} \cos\theta + \dot{\psi}, \\ \omega_2 &\equiv \dot{\theta} \sin\psi - \dot{\varphi} \sin\theta \cos\psi, \\ \omega_3 &\equiv \dot{\theta} \cos\psi + \dot{\varphi} \sin\theta \sin\psi. \end{aligned}\right\} \quad (2\text{-D})$$

The quantities A_x, A_y, A_z are given by

$$A_x = \frac{16\pi\mu}{3(b^2\beta_0 + b^2\gamma_0)},$$

$$A_y = \frac{16\pi\mu}{3(b^2\gamma_0 + a^2\alpha_0)},$$

and

$$A_z = \frac{16\pi\mu}{3(a^2\alpha_0 + b^2\beta_0)}, \quad (3\text{-D})$$

where

$$\left.\begin{aligned}
\beta_0 = \gamma_0 &= \frac{a}{(a^2-b^2)(b^2)} - \frac{1}{2(a^2-b^2)^{3/2}} \log_e\left|\frac{\sqrt{a^2-b^2}+a}{\sqrt{a^2-b^2}-a}\right| \\
&\text{and} \\
\alpha_0 &= \frac{2}{(a^2-b^2)}\left\{\frac{1}{2(a^2-b^2)^{1/2}} \log_e\left|\frac{\sqrt{a^2-b^2}+a}{\sqrt{a^2-b^2}-a}\right| - \frac{1}{a}\right\}.
\end{aligned}\right\} \quad (4\text{-D})$$

APPENDIX E

DERIVATION OF ORIENTATION DISTRIBUTION FUNCTION FOR COMBINED KERR AND MAXWELL EFFECTS

We seek solutions of the equation

$$\nabla^2 F = -\frac{A}{D}(3\sin^2\theta \sin 2\gamma + [3\cos^2\theta - 1]\sin 2\lambda)F$$

$$+ \frac{A}{2D}\sin 2\theta\,(\sin 2\gamma - \sin 2\lambda)\frac{\partial F}{\partial \theta}$$

$$+ \frac{A}{D}(\cos 2\gamma + \frac{\cos 2\lambda}{R})\frac{\partial F}{\partial \gamma} \qquad (1\text{-E})$$

where

$$\nabla^2 = \frac{1}{\sin\theta}\frac{\partial}{\partial\theta}(\sin\theta\frac{\partial}{\partial\theta}) + \frac{1}{\sin^2\theta}\frac{\partial^2}{\partial\gamma^2},$$

F = distribution function,

2λ = a constant defined by $M = A\sin 2\lambda$ and $2K = A\cos 2\lambda$

where $K = \frac{1}{4}G\left(\frac{a^2-b^2}{a^2+b^2}\right)$ and $M = \frac{1}{A_y}\left(\frac{BE^2}{a^2+b^2}\right)$,

$$R = \left(\frac{a^2-b^2}{a^2+b^2}\right),$$

and

D = rotary diffusion coefficient.

Let $\frac{A}{D} \equiv \beta$ and let F be repressnted by the series

$$F = \sum_{j=0}^{\infty} \beta^j F_j. \qquad (2\text{-E})$$

Then F_j satisfies the inhomogeneous equation:

$$\nabla^2 F_j = -(3 \sin^2\theta \sin 2\gamma + [3 \cos^2\theta - 1] \sin 2\lambda)F_{j-1}$$

$$+ \frac{1}{2} \sin 2\theta (\sin 2\gamma - \sin 2\lambda) \frac{\partial F_{j-1}}{\partial \theta}$$

$$+ (\cos 2\gamma + \frac{1}{R} \cos 2\lambda) \frac{\partial F_{j-1}}{\partial \gamma} \, . \qquad (3\text{-E})$$

Here F_j may be expressed in terms of a series of spherical harmonics as

$$F_j = \frac{1}{2} \sum_{n=0}^{\infty} a_{n0,j} P_{2n} + \sum_{n=1}^{\infty} \sum_{m=1}^{n} (a_{nm,j} \cos 2m\gamma + b_{nm,j} \sin 2m\gamma) P_{2n}^{2m} \qquad (4\text{-E})$$

where $a_{n0,j}$, $a_{nm,j}$, $b_{nm,j}$ are the appropriate coefficients, P_{2n} are the appropriate Legendre polynomials and P_{2n}^{2m} are the appropriate Legendre functions.

Now observe that the coefficients of equation 3-E may be expressed as

$$3 \sin^2\theta \sin 2\gamma + [3 \cos^2\theta - 1] \sin 2\lambda \equiv P_2^2 \sin 2\gamma + 2P_2 \sin 2\lambda$$

$$\frac{1}{2} \sin 2\theta \equiv \frac{1}{3} P_2^1 \qquad (5\text{-E})$$

Then equation 3-E becomes

$$\nabla^2 F_j = -(P_2^2 \sin 2\gamma + 2P_2 \sin 2\lambda)F_{j-1}$$

$$+ \frac{1}{3} P_2^1 (\sin 2\gamma - \sin 2\lambda) \frac{\partial F_{j-1}}{\partial \theta}$$

$$+ (\cos 2\gamma + \frac{1}{R} \cos 2\lambda) \frac{\partial F_{j-1}}{\partial \gamma} \qquad (6\text{-E})$$

Note that equation 4-E yields

$$\frac{\partial F_{j-1}}{\partial \theta} = -\frac{1}{2} \sum_{n=0}^{\infty} a_{n0,j} P_{2n}^1 + \sum_{n=1}^{\infty} \sum_{m=1}^{n} (a_{nm,j-1} \cos 2m\gamma$$

$$+ b_{nm,j-1} \sin 2m\gamma)(2m \cot \theta P_{2n}^{2m} - P_{2n}^{2m+1}) \qquad (7\text{-E})$$

and

$$\frac{\partial F_{j-1}}{\partial \gamma} = \sum_{n=1}^{\infty} \sum_{m=1}^{n} (-2ma_{nm,j-1}\sin 2m\gamma + 2mb_{nm,j-1}\cos 2m\gamma)P_{2n}^{2m} \qquad (8\text{-E})$$

where

$$P_{2n}^{2m+1} = 0 \text{ when } m = n.$$

The functions F_j, $\frac{\partial F_j}{\partial \theta}$, $\frac{\partial F_j}{\partial \gamma}$ can now be expressed in terms of Legendre functions and polynomials. They appear in Tables 1, 2 and 3 of this Appendix. The coefficients are computed as follows: From equation 3-E we obtain

$$\left.\begin{aligned} \nabla^2 F_0 &= 0 \\ \nabla^2 F_1 &= f_1 F_0 + f_2 \frac{\partial F_0}{\partial \theta} + f_3 \frac{\partial F_0}{\partial \gamma} \\ \nabla^2 F_2 &= f_1 F_1 + f_2 \frac{\partial F_1}{\partial \theta} + f_3 \frac{\partial F_1}{\partial \gamma} \\ &\vdots \end{aligned}\right\} \qquad (9\text{-E})$$

where f_1, f_2 and f_3 are equal to $(P_2^2 \sin 2\gamma + 2P_2 \sin 2\lambda)$, $\frac{1}{3} P_2^1(\sin 2\gamma - \sin 2\lambda)$ and $(\cos 2\gamma + \frac{1}{R} \cos 2\lambda)$ respectively.

Noting that each F_j is a series of spherical harmonics, we obtain for the left-hand side of equations 9-E,

$$\left.\begin{aligned} \nabla^2 F_0 &= -\sum_{n}^{\infty} 2n(2n+1)F_{0n} \\ \nabla^2 F_1 &= -\sum_{n}^{\infty} 2n(2n+1)F_{1n} \\ &\vdots \end{aligned}\right\} \qquad (10\text{-E})$$

where

$$F_{jn} = \frac{1}{2} a_{n0,j} P_{2n} + \sum_{m=1}^{n} (a_{nm,j} \cos 2m\gamma + b_{nm,j} \sin 2m\gamma) P_{2n}^{2m} \qquad (11\text{-E})$$

and j = 0, 1, 2... while n = 0, 1, 2... .

We may now form the equations

$$\left.\begin{aligned} -\sum_{n}^{\infty} 2n(2n+1)F_{0n} &= 0 \\ -\sum_{n}^{\infty} 2n(2n+1)F_{1n} &= f_1 F_0 + f_2 \frac{\partial F_0}{\partial \theta} + f_3 \frac{\partial F_0}{\partial \gamma} \\ -\sum_{n}^{\infty} 2n(2n+1)F_{2n} &= f_1 F_1 + f_2 \frac{\partial F_1}{\partial \theta} + f_3 \frac{\partial F_1}{\partial \gamma} \\ &\vdots \end{aligned}\right\} \qquad (12\text{-E})$$

and with the aid of Tables 1, 2 and 3 of this Appendix we may express equation 11-E in terms of the coefficients $a_{nm,j}$ and $b_{nm,j}$. We may then equate the coefficients of the terms $x^P \sin 2q\gamma$ and $x^P \cos 2q\gamma$ on either side and solve for $a_{nm,j}$ and $b_{nm,j}$ in terms of $a_{00,0}$. The value of $a_{00,0}$ is obtained by normalization of the integral $\int F\, d\Omega$ to unity, where $d\Omega$ is the solid angle $\sin\theta d\theta d\varphi$ and the limits are 0 to 2π for φ and 0 to π for θ (or -2λ to $2\pi - 2\lambda$ for $2\gamma = 2\varphi - 2\lambda$). Since each F_j is orthogonal to all the others and since $\sin\theta = P_1^1$, if the integration of, say, the first term over the solid angle, i.e.

$$\int_0^{2\pi} \int_0^{\pi} F_0 P_1^1 \, d\theta d\varphi$$

yields a finite value, this is sufficient proof that all the other integrals must vanish, i.e.

$$\int_0^{2\pi}\int_0^{\pi} F_0 P_1^1 \, d\theta d\varphi = 0, \text{ for } j > 0,$$

since these F_j terms are then orthogonal to P_1^1.

We may now proceed to compute the first few terms of equation 2-E.

A. COMPUTATION OF FIRST TERM

From the first equation of the set of equations 9-E, and from the discussion preceding equation 6 of the text we conclude that F_0 is a constant equal to $\frac{1}{2} a_{00,0}$ and that $F_0 = \frac{1}{4\pi}$. Therefore we obtain

$$F_0 = \frac{1}{2} a_{00,0}, \tag{13-E}$$

and

$$a_{00,0} = \frac{1}{2\pi}. \tag{14-E}$$

This can also be shown by carrying out the operations indicated by equations 9-E and 11-E, computing F_0 and inserting it into equation 41 of the text.

B. COMPUTATION OF SECOND TERM

Since

$$F_0 = \frac{1}{2} a_{00,0} = \text{constant},$$

we obtain

$$\frac{\partial F_0}{\partial \theta} = \frac{\partial F_0}{\partial \gamma} = 0.$$

Therefore

$$-\sum_n^{\infty} 2n(2n+1)F_{1n} = f_1 F_0 \; ; \quad n = 0,1,2,\ldots$$

Since $P_2^2 = 3\sin^2\theta$ and $2P_2 = 3\cos^2\theta - 1$, the right-hand side becomes

$$-\ (P_2^2 \sin 2\gamma + 2P_2 \sin 2\lambda)\ \frac{1}{2}\ a_{00,0}$$

and the left-hand side becomes

$$-0 \times a_{00,1} + (-2)(3)\ \frac{1}{2}\ a_{10,1}P_2 + (-2)(3)(a_{11,1}\cos 2\gamma + b_{11,1}\sin 2\gamma)P_2^2$$
$$+ (-4)(5)[\ \frac{1}{2}\ a_{20,1}P_4 + (\ )P_4^2 + (\ )P_4^4\ ] + \ldots$$

+ terms which contain $P^q_{4+\ell}$ and therefore need not appear.

Since the right-hand side contains only P_2^2 and P_2, we discard all terms higher than that, i.e.

$$a_{nm,1} = b_{nm,1} = 0 \text{ except for } n = 1 \begin{cases} m=0 \\ m=1 \end{cases} .$$

Therefore

$$-3a_{10,1}P_2 - 6(a_{11,1}\cos 2\gamma + b_{11,1}\sin 2\gamma)P_2^2$$
$$= -\ (P_2^2 \sin 2\gamma + 2P_2 \sin 2\lambda)\ \frac{1}{2}\ a_{00,0}\ .$$

Hence

$$a_{10,1} = \frac{a_{00,0}}{3} \sin 2\lambda, \quad a_{11,1} = 0$$

and

$$b_{11,1} = \frac{1}{12}\ a_{00,0}. \qquad (15\text{-E})$$

C. COMPUTATION OF THIRD TERM

The third term coefficients are best derived by expressing the Legendre polynomials and functions in terms of x (i.e. $P_1 = x$, $P_1^1 = (1-x^2)^{1/2}$), $x^P \sin 2q\gamma$ and $x^P \cos 2q\gamma$, and comparing terms as outlined in the text under the discussion for the general term. That yields a system of 8 simultaneous equations, with solutions:

$$\left.\begin{aligned}
a_{10,2} &= \frac{1}{7}\left(-\frac{1}{3}+\frac{1}{9}\sin^2 2\lambda\right)a_{00,0} \\
a_{20,2} &= \frac{1}{70}\left(1+2\sin^2 2\lambda\right)a_{00,0} \\
a_{11,2} &= -\frac{1}{36R}(\cos 2\lambda)a_{00,0} \\
a_{21,2} &= 0 \\
a_{22,2} &= -\frac{1}{3\cdot4\cdot5\cdot7\cdot8}a_{00,0} \\
b_{11,2} &= -\frac{1}{126}(\sin 2\lambda)a_{00,0} \\
b_{21,2} &= \frac{1}{420}(\sin 2\lambda)a_{00,0} \\
b_{22,2} &= 0.
\end{aligned}\right\} \quad (16\text{-E})$$

TABLE 1

THE FIRST FEW TERMS F_j AS FUNCTIONS OF n AND j

$j \backslash n$	0	1	2	3
0	$\frac{1}{2} a_{00,0}$	$\frac{1}{2} a_{10,0} P_2$ $+ (a_{11,0} \cos 2\gamma + b_{11,0} \sin 2\gamma) P_2^2$	$\frac{1}{2} a_{20,0} P_4$ $+ (a_{21,0} \cos 2\gamma + b_{21,0} \sin 2\gamma) P_4^2$ $+ (a_{22,0} \cos 4\gamma + b_{22,0} \sin 4\gamma) P_4^4$	...
1	$\frac{1}{2} a_{00,1}$	$\frac{1}{2} a_{10,1} P_2$ $+ (a_{11,1} \cos 2\gamma + b_{11,1} \sin 2\gamma) P_2^2$	$\frac{1}{2} a_{20,1} P_4$ $+ (a_{21,1} \cos 2\gamma + b_{21,1} \sin 2\gamma) P_4^2$ $+ (a_{22,1} \cos 4\gamma + b_{22,1} \sin 4\gamma) P_4^4$	...
2	$\frac{1}{2} a_{00,2}$	$\frac{1}{2} a_{10,2} P_2$ $+ (a_{11,2} \cos 2\gamma + b_{11,2} \sin 2\gamma) P_2^2$	$\frac{1}{2} a_{20,2} P_4$ $+ (a_{21,2} \cos 2\gamma + b_{21,2} \sin 2\gamma) P_4^2$ $+ (a_{22,2} \cos 4\gamma + b_{22,2} \sin 4\gamma) P_4^4$	...
3	⋮	⋮	⋮	⋮

TABLE 2

THE FIRST FEW TERMS $\frac{\partial F_{j-1}}{\partial \theta}$ AS FUNCTIONS OF n AND j

j-1 \ n	j	0	1	2	3
-1	0	0	$-\frac{1}{2} a_{10,0} P_2^1$ $+(a_{11,0} \cos 2\gamma + b_{11,0} \sin 2\gamma)(2\cot\theta\, P_2^2)$	$-\frac{1}{2} a_{20,0} P_4^1$ $+(a_{21,0} \cos 2\gamma + b_{21,0} \sin 2\gamma)(2\cot\theta\, P_4^2 - P_4^3)$ $+(a_{22,0} \cos 4\gamma + b_{22,0} \sin 4\gamma)(4\cot\theta\, P_4^4)$	...
0	1	0	$-\frac{1}{2} a_{10,1} P_2^1$ $+(a_{11,1} \cos 2\gamma + b_{11,1} \sin 2\gamma)(2\cot\theta\, P_2^2)$	$-\frac{1}{2} a_{20,1} P_4^1$ $+(a_{21,1} \cos 2\gamma + b_{21,1} \sin 2\gamma)(2\cot\theta\, P_4^2 - P_4^3)$ $+(a_{22,1} \cos 4\gamma + b_{22,1} \sin 4\gamma)(4\cot\theta\, P_4^4)$	...
1	2	0	$-\frac{1}{2} a_{10,2} P_2^1$ $+(a_{11,2} \cos 2\gamma + b_{11,2} \cos 2\gamma)(2\cot\theta\, P_2^2)$	$-\frac{1}{2} a_{20,2} P_4^1$ $+(a_{21,2} \cos 2\gamma + b_{21,2} \sin 2\gamma)(2\cot\theta\, P_4^2 - P_4^3)$ $+(a_{22,2} \cos 4\gamma + b_{22,2} \sin 4\gamma)(4\cot\theta\, P_4^4)$	...
		0	⋮	⋮	⋮

TABLE 3

THE FIRST FEW TERMS $\frac{\partial F_{j-1}}{\partial \gamma}$ AS FUNCTIONS OF n AND j

j-1 \ n	j	0	1	2	3
-1	0	0	$(-2a_{11,0}\sin 2\gamma + 2b_{11,0}\cos 2\gamma)P_2^2$	$(-2a_{21,0}\sin 2\gamma + 2b_{21,0}\cos 2\gamma)P_4^2$ $+ (-4a_{22,0}\sin 4\gamma + 4b_{22,0}\cos 4\gamma)P_4^4$	...
0	1	0	$(-2a_{11,1}\sin 2\gamma + 2b_{11,1}\cos 2\gamma)P_2^2$	$(-2a_{21,1}\sin 2\gamma + 2b_{21,1}\cos 2\gamma)P_4^2$ $+ (-4a_{22,1}\sin 4\gamma + 4b_{22,1}\cos 4\gamma)P_4^4$	...
1	2	0	$(-2a_{11,2}\sin 2\gamma + 2b_{11,2}\cos 2\gamma)P_2^2$	$(-2a_{21,2}\sin 2\gamma + 2b_{21,2}\cos 2\gamma)P_4^2$ $+ (-4a_{22,2}\sin 4\gamma + 4b_{22,2}\cos 4\gamma)P_4^4$	...
		⋮	⋮	⋮	⋮

APPENDIX F

DESCRIPTION OF APPARATUS AND PROCEDURES

Conceptually, the design of this apparatus for measuring streaming birefringence does not differ from that of Edsall, Rich and Goldstein (26). It consists of two concentric cylinders mounted one inside the other with the outer cylinder rotating. (Taylor (21,22) was first to point out that with this arrangement higher velocity gradients can be obtained with relatively large annular gaps before the onset of turbulence.) However, a large number of improvements were incorporated into the design of this instrument. In addition the stator was electrically insulated from the rotor and the rest of the apparatus in order to make possible the application of a potential across the annular gap for the experimental study of the effect of electrostatic fields on the orientation of colloidal particles immersed in Couette flow.

The large number of delicate manipulations required to operate previous versions of SBR equipment indicated that considerable thought should be given to methods for simplifying and speeding up the operation of this apparatus. At the same time it was decided to improve the operating characteristics and extend the range of gradients over which SBR measurements could be made.

Thus it was decided to place the high-voltage water-cooled mercury arc light source out of the way and for this purpose a wooden shelf was constructed over the bench on which stands the rest of the equipment. In order to facilitate loading and cleaning the annular gap and in order to improve the accessibility of the drive mechanism it was decided to mount all the mechanical parts on one housing. This housing in turn was mounted on a sturdy vertical stand in such a way that it can be lowered or lifted and rotated at will. This gave considerable freedom of movement to the test area. Finally, the optical parts were mounted on another vertical stand which can slide back and forth on rails in the direction of the stand supporting the mechanical parts. A special mechanism was provided for rotating the Glan-Thompson polarizing prisms individually and for clamping them together so that they rotate while their optical axes remain at a fixed angle with each other. The supports of the prisms are fixed on the same frame and this frame can slide up and down on the optical stand or rotate around it. Thus the optical system can follow and survey the annular gap between the rotor and stator at any required position. Clamps are provided to lock and secure the optical stand at any required position on the rails, and the two sliding frames (housing the motors and the prisms) at any required position on the vertical stands.

In order to assure an extensive range of velocity gradients with smooth (i.e. constant-speed and vibrationless operation) two motors were provided to drive the rotor. For low speeds the rotor is driven through a geared 1/15 HP motor and for high speeds the rotor is driven directly by a 1/4 HP motor. The speed of both motors can be varied and controlled through an electronic regulator. A V-belt is provided to drive the rotor and by rotating the motor housing the appropriate motor can be selected.

To measure the rate of rotation a geared wheel was attached to the rotor and a magnetic pickup was provided to sense the rate at which the teeth of the gear pass a given spot. Holes are provided on the stator for inserting thermocouples to measure the temperature of the fluid. The stator is insulated from the rotor so that a potential can be applied across the annular gap.

A complete set of mechanical drawings of this equipment exists at the California Institute of Technology Central Shop under Work Orders 386 and 15003, drawings No. 1051-1132, Aug. 1956-Aug. 1957.

1. Description of Apparatus

The present design (see figure 1, Appendix F) consists of three main pieces: A horizontal optical bench (1), overhead, containing the light-source (1a), collimator (1b) and 90° prism (1c); a vertical optical bench (2), containing the Glan-Thompson prisms (7), appropriate fine collimator (2a) and eyepiece (2b); and a vertical stand (3), containing the rotor and stator assembly (5,6) and the motors required to operate it (4a,4d). The entire weight of the two vertical stands is supported on a sturdy wooden bench (14).

The light source (1a) is a water-cooled mercury arc. This is a high-intensity arc. It is necessary to operate it through a high-voltage power supply (not shown here). The second adjustable and movable collimator (2a) contains a pinhole apperture followed by a condensing lens for focusing the resulting thin ray of light approximately half-way down the gap between the two cylinders. The thin pencil of light begins to spread somewhat after it is halfway down the gap but since the focal length of the lens is long (1 m) compared with the dimensions involved here, the light beam does not spread too much before it reaches the eyepiece (2b). The intensity of the light beam may be

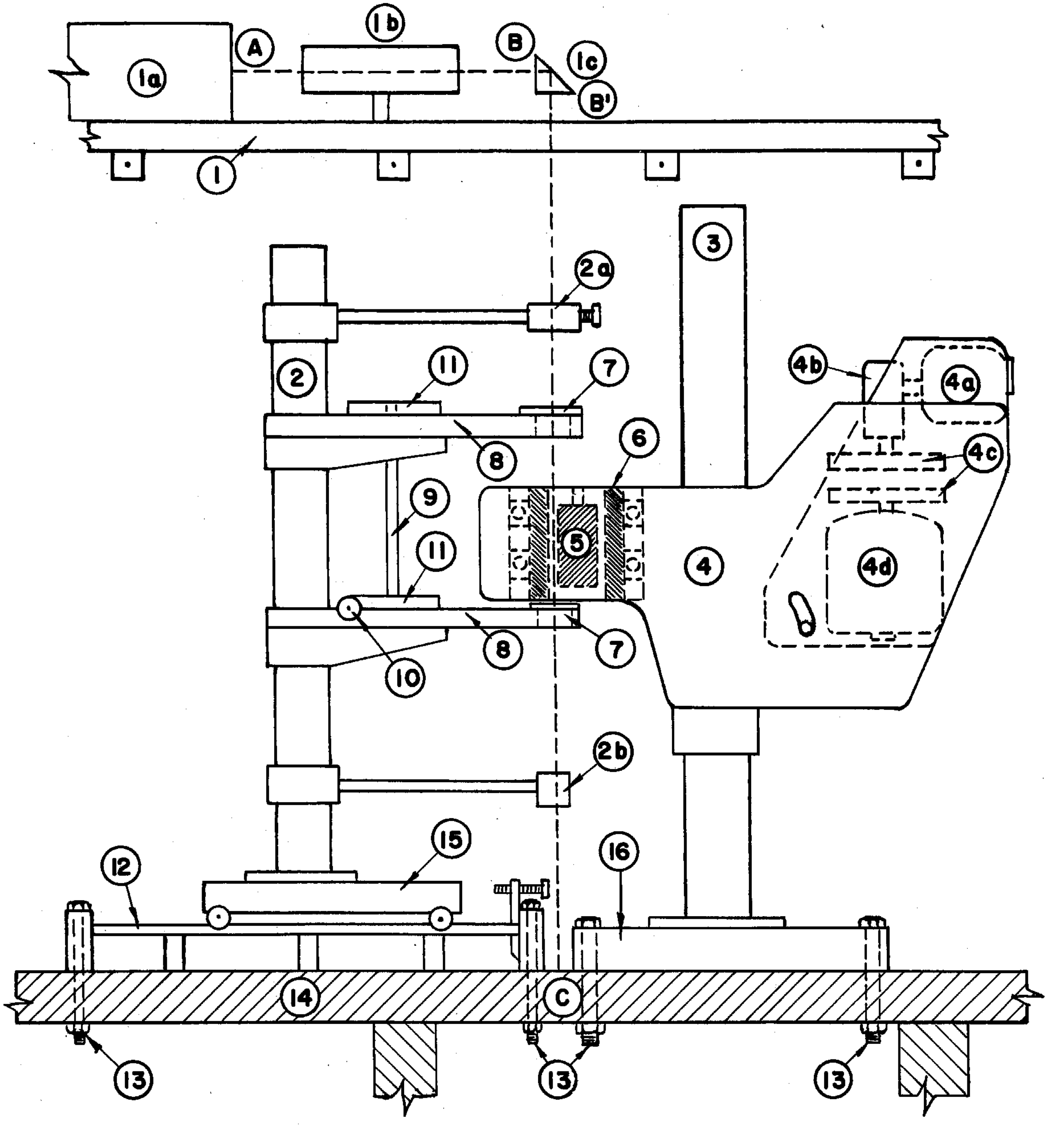

Figure 1, APPENDIX F

SCHEMATIC OF IMPROVED SBR APPARATUS

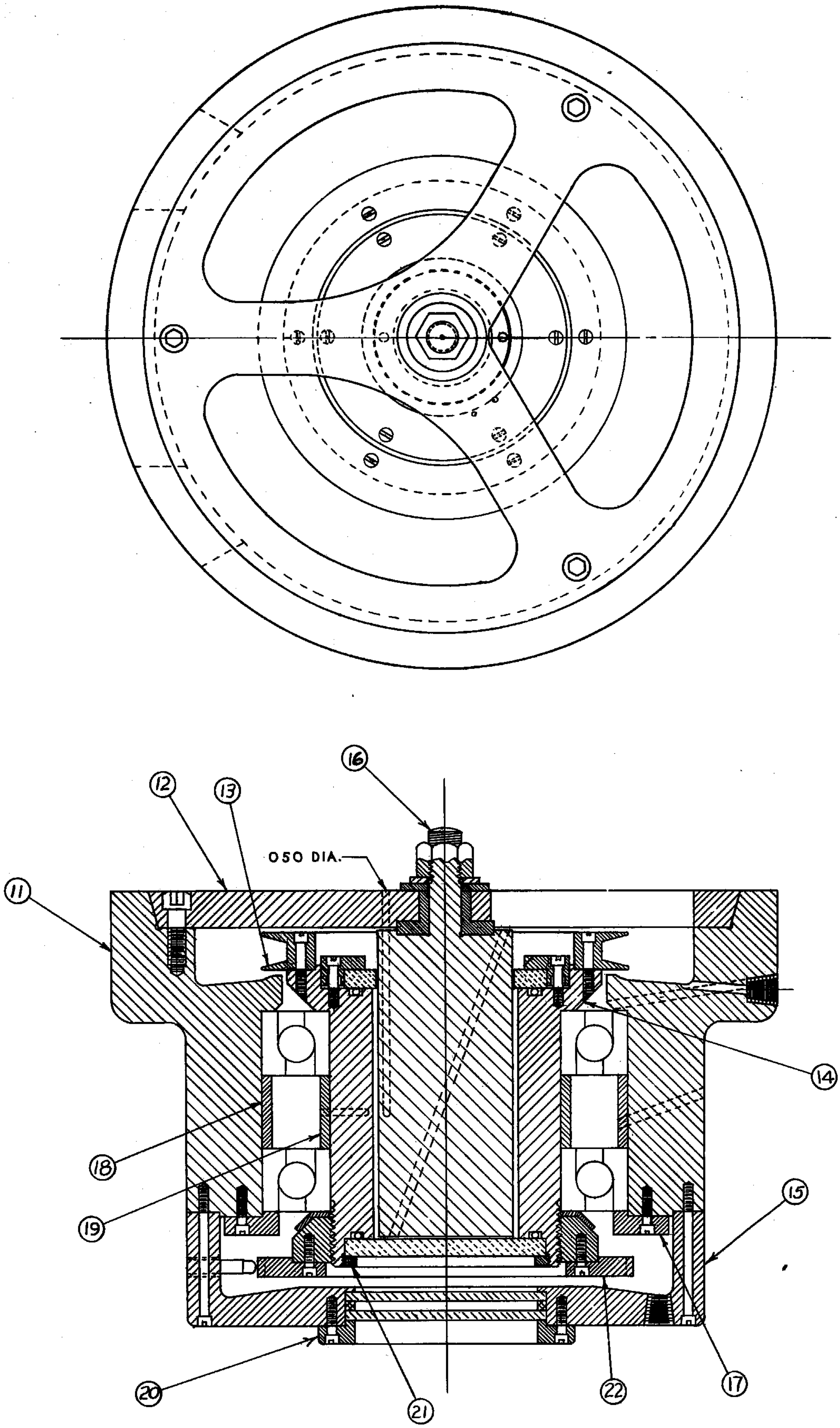

FIGURE 2, APPENDIX F
ROTOR AND STATOR ASSEMBLY (VERSION I)

improved by inserting a lens just after the collimator (1b) to focus the light beam on the pinhole of collimator (2a).

A drawing of the first version of the rotor and stator assembly is shown in figure 2, Appendix F. The narrow gap between the optically-flat and stress-free upper window and the stator was a source of trouble repeatedly. The reason for the existence of this gap is the need to anchor the optical upper window to the outer cylinder, which is rotating. The width of the gap is dictated by two main considerations: the upper window must be far enough from the stator wall so that the rotating glass does not scrape against the stator and it must be close enough to the stator so that no fluid leaks upward and the stream can be surveyed as close to the stator as possible. Therefore a fine fit around the stator is required. The first version of this gap is shown in detail in figure 3, Appendix F.

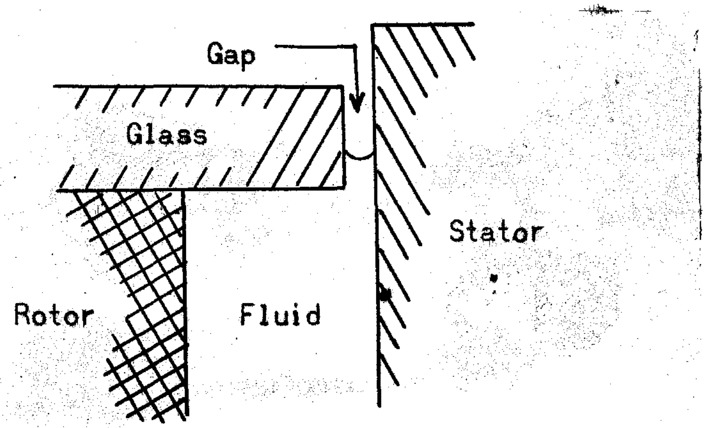

FIGURE 3, APPENDIX F
DETAIL OF GAP BETWEEN UPPER GLASS WINDOW AND STATOR -- FIRST VERSION

However, this fine fit was found to cause the chipping of the unprotected inner edge of the annular upper window whenever the window edge touched the stator during the assembly and adjustment of the system.

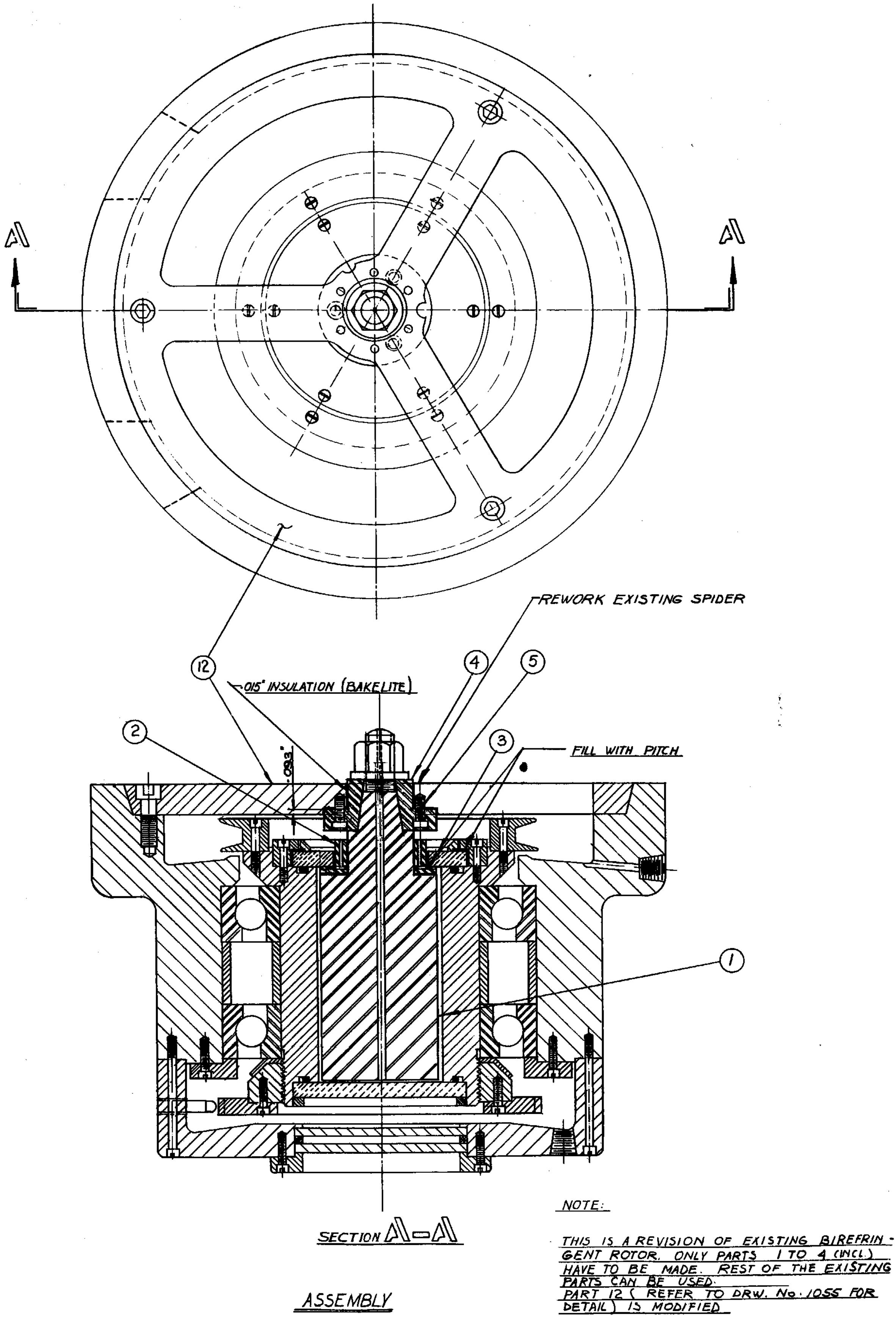

FIGURE 4, APPENDIX F

ROTOR AND STATOR ASSEMBLY (VERSION II)

Since the heavy stator had to be moved up past this narrow gap frequently in order to clean the interior of the system, it was found necessary to re-design that part of the equipment.

A second source of trouble originating at the upper window was the inability of the small bubbles of air, that formed during the filling of the gap with fluid, to escape past the narrow gap between the window and the stator. These bubbles rotated with the upper window and destroyed the uniformity of the beam by refraction and reflection.

For these reasons it was found necessary to evolve the design of the rotor and stator assembly shown in figure 4, Appendix F. A detail of the second version of the gap is shown in figure 5, Appendix F.

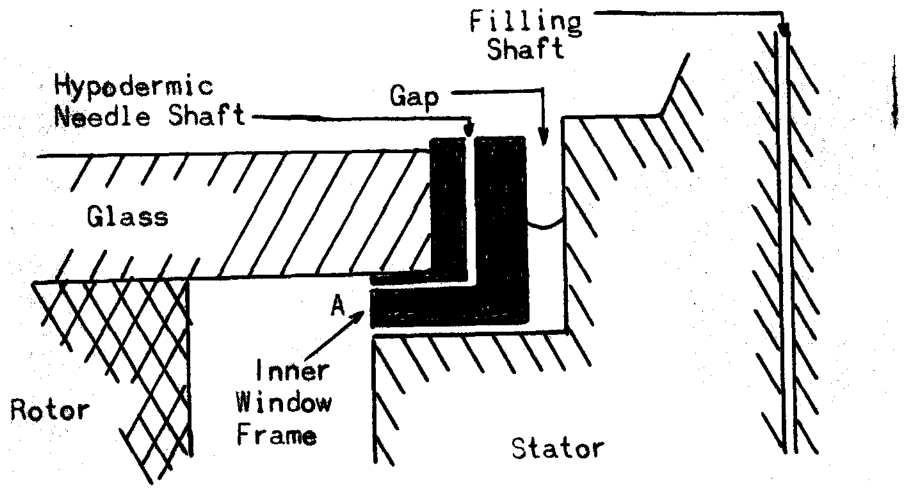

FIGURE 5, APPENDIX F
DETAILS OF GAP BETWEEN UPPER GLASS WINDOW AND STATOR -- SECOND VERSION

It was found necessary to indent the stator and fit a stainless-steel ring around the inner edge of the glass window. The window was seated on this ring and fixed there with pitch. Holes, (A), were provided in 6 places around the perimeter of this inner window frame and these holes were connected to vertical shafts through which a hypodermic needle could be inserted to suck out any air bubbles that might form. Although this version finally worked adequately, it was found in subsequent experiments suggested by Prof. J. H. Wayland and performed by S. Sutera that the entire inner window frame could be removed without introducing any adverse effects in the experiment (except for a small gradient at the upper inner edge), provided the shaft for filling the gap with fluid remains sealed. It appears therefore that the design of the gap can be further improved by bringing the ledge of the stator closer to the lower edge of the upper window, as shown in figure 6, Appendix F.

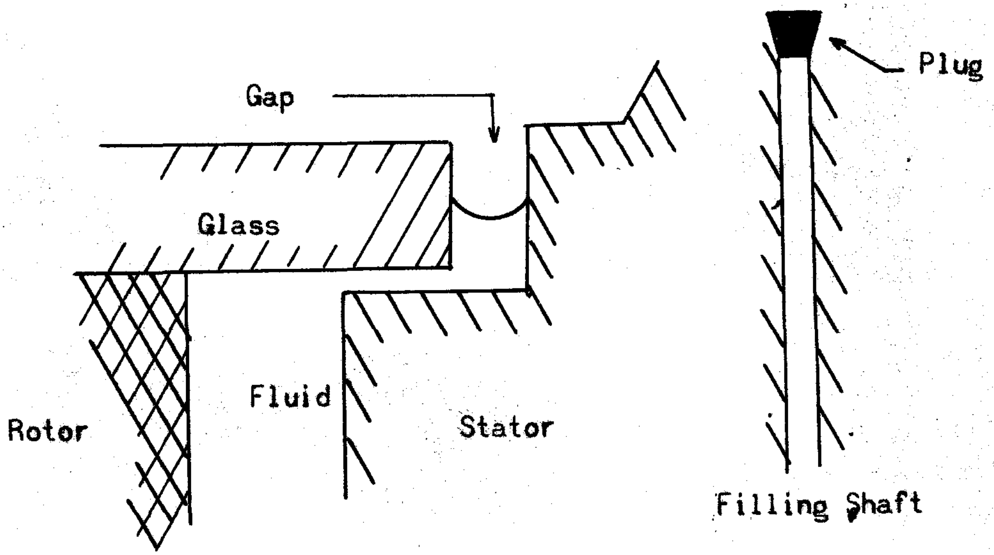

FIGURE 6, APPENDIX F
DETAIL OF RECOMMENDED DESIGN OF GAP

The indented stator assembly which has been found successful is shown in figure 7, Appendix F. The rotor and stator assembly is shown

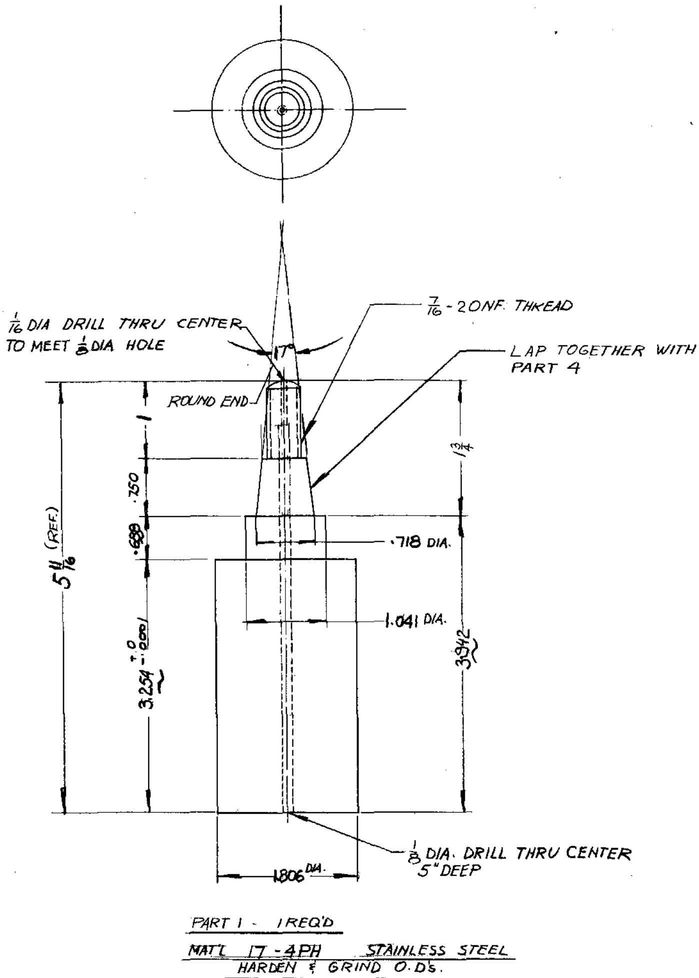

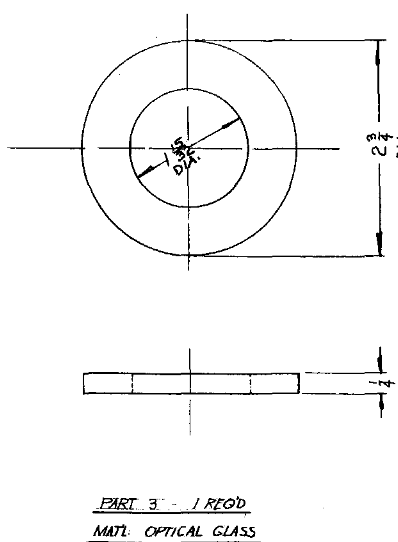

FIGURE 7, APPENDIX F
STATOR ASSEMBLY
(VERSION II)

in figure 8, Appendix F. The optical frame for the rotation of the Glan-Thompson prisms simultaneously or individually, is shown in figure 9, Appendix F. The assembled streaming birefringence apparatus is shown in figure 10, Appendix F.

2. Procedure

The first and perhaps most critical step in measuring streaming birefringence consists of aligning the apparatus correctly. Thus it is absolutely necessary that the light beam BC (see figure 1, Appendix F) be perpendicular to all glass surfaces (lenses in collimator (2a), upper Glan-Thompson prism (7), upper and lower window of gap between cylinders, lower Glan-Thompson prism (7) and eyepiece prism (2b)). To insure this, it is necessary to carry out the following steps:

(a) Insert slivers of metal under the base (16), of the SBR stand (3) and tighten the anchoring bolts (13), until a level resting on the rotor and stator assembly shows that the top of that assembly is horizontal. Move the level around to different positions and make sure the top of the assembly has no tilt. When this is accomplished, the walls of the gap and the axes of the concentric cylinders should be vertical.

(b) Repeat this with base (12a) of stand (2), resting the level on the top frame (8). Make sure that the rails (12) are sufficiently close to the other stand to permit surveying the gap on all sides of the stator.

(c) Once the stands (2) and (3) are firmly in place, drop a plumb-line from a point on the lower surface of the prism (1c) through the gap between rotor and stator to point C. Then adjust the orientation of the

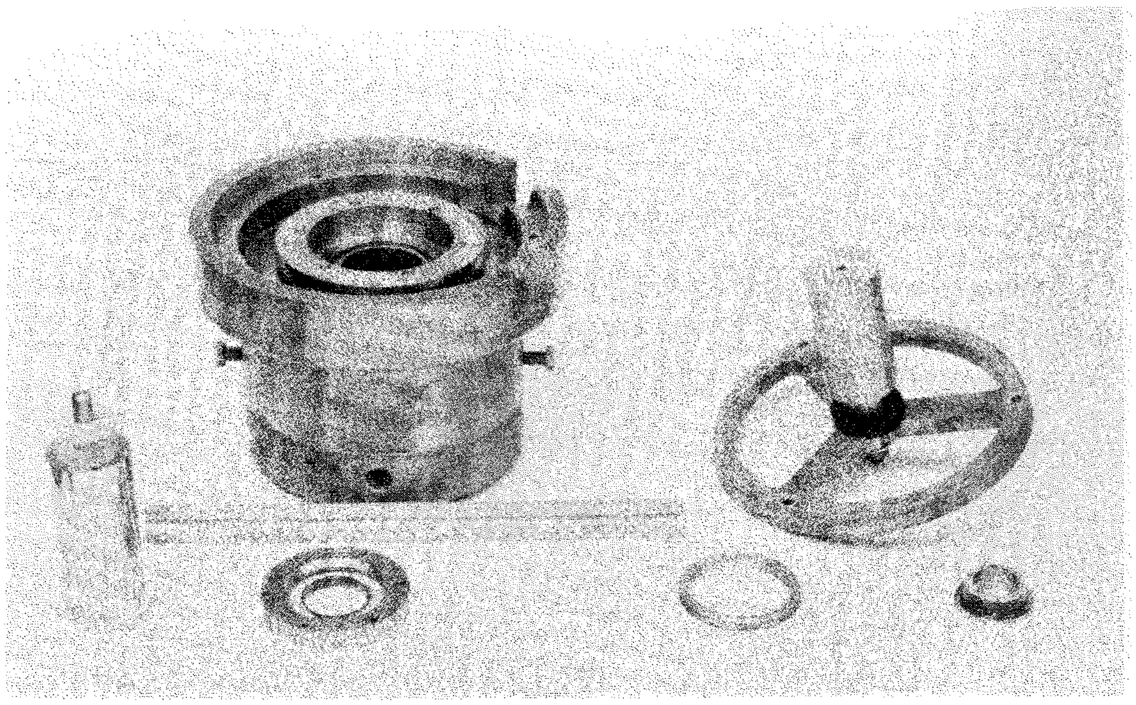

FIGURE 8, APPENDIX F
PHOTOGRAPH OF ROTOR AND STATOR ASSEMBLY

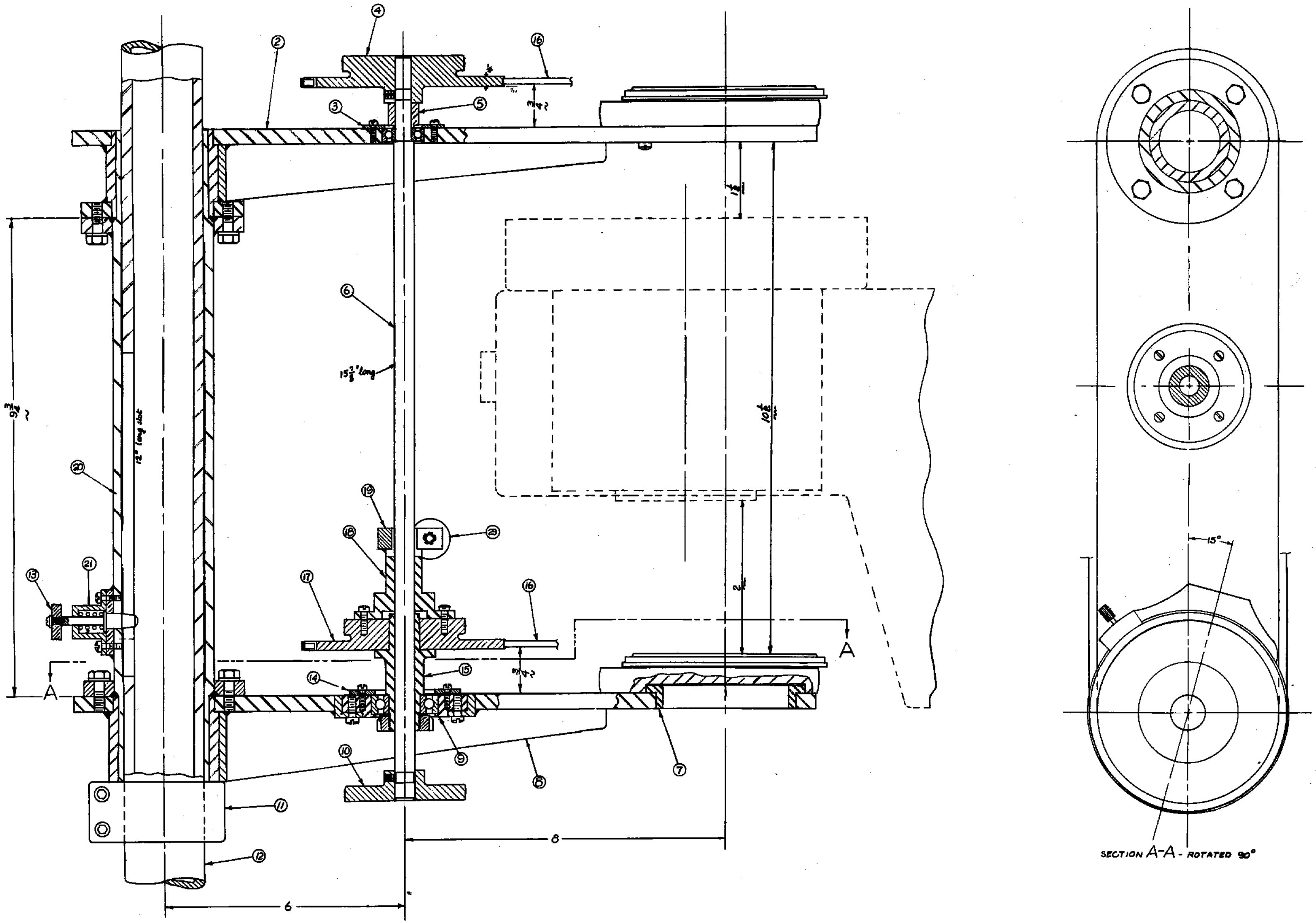

FIGURE 9, APPENDIX F
OPTICAL FRAME FOR GLAN-THOMPSON PRISMS

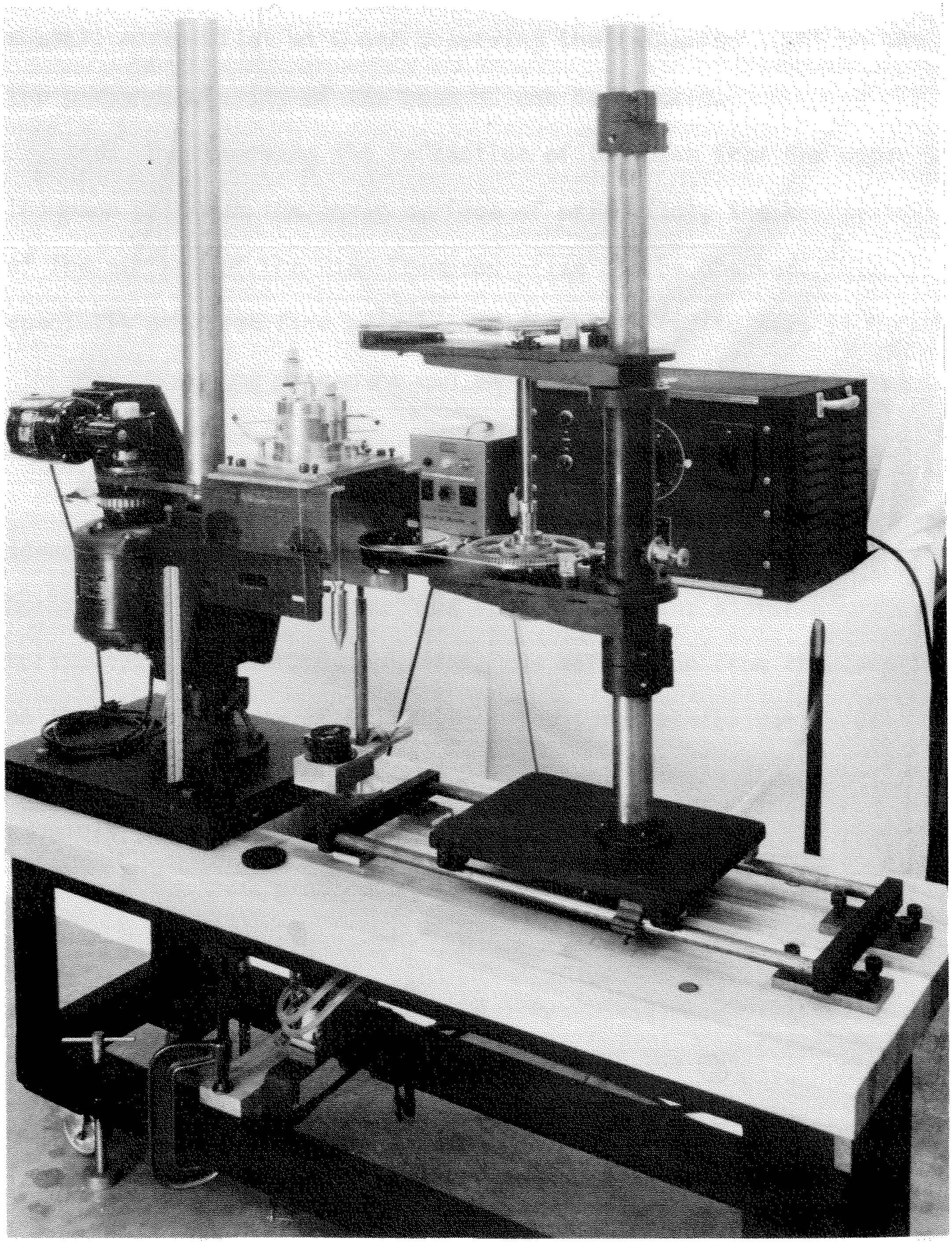

FIGURE 10, APPENDIX F

PHOTOGRAPH OF ASSEMBLED STREAMING BIREFRINGENCE APPARATUS (WITH ECCENTRIC CYLINDERS MOUNTED) prism so that the reflected light beam follows that path. By putting a small mirror flat at C and observing the reflected light on the prism, the perpendicularity of the beam BC can be checked.

(d) By observing the reflection of the beam from the upper Glan-Thompson prism on the lower surface of prism (lc), the horizontality of the surface of the Glan-Thompson prism can be checked. Use the specially provided fine adjustments on the latter to make it horizontal.

(e) The same procedure can be repeated with the lower Glan-Thompson prism.

(f) The rotor and stator assembly has been designed so that the lower window of the gap should be perpendicular to the light beam (i.e. horizontal) if the upper surface of the rotor and stator assembly is horizontal. However, by observing the reflection from the lower window on the lower surface of prism (lc), the lower window can be adjusted (by shaving off portions of the O-ring seal between it and the rotor assembly) so that it is perpendicular to the beam.

(g) The same procedure is repeated with the upper window which can be adjusted by tightening the screws holding it in place against the rotor. This procedure insures the correct alignment of the instruments and the walls of the gap: The axes of the cylinders are parallel to the light beam and all optical surfaces are perpendicular to the light beam.

(h) The apparatus is now ready to be filled with the working fluid. This can be done by unclamping the optical stand and rolling it away. This exposes the filling shaft. The fluid is inserted with a hypodermic needle from a 20 cc syringe.

(i) The optical stand is rolled back on and the correct motor speed is chosen. The motor is started and one final check is made for bubbles and for the correct alignment of the optical surfaces (by making sure no multiple and revolving reflections appear on the lower surface of the prism (1c)).

(j) The temperature is checked by reading the thermocouple voltage.

The rest of the procedure for SBR measurements follows closely that described in reference 3. A voltage may be applied across the gap by attaching the electrodes on the appropriate connection on the rotor and the insulated stator.